Magnetic Resonance with Single Nuclear-Spin Sensitivity

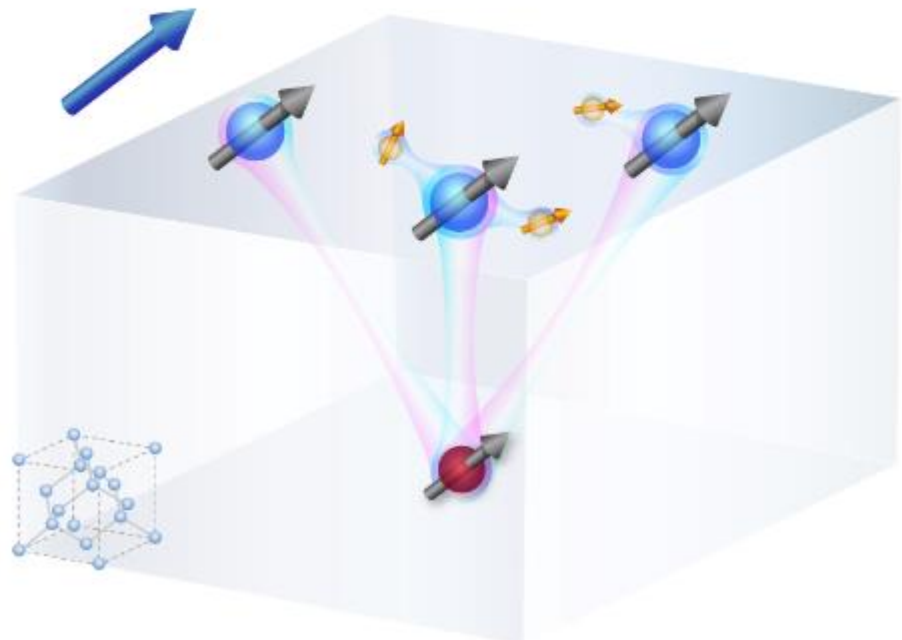

Alex Sushkov

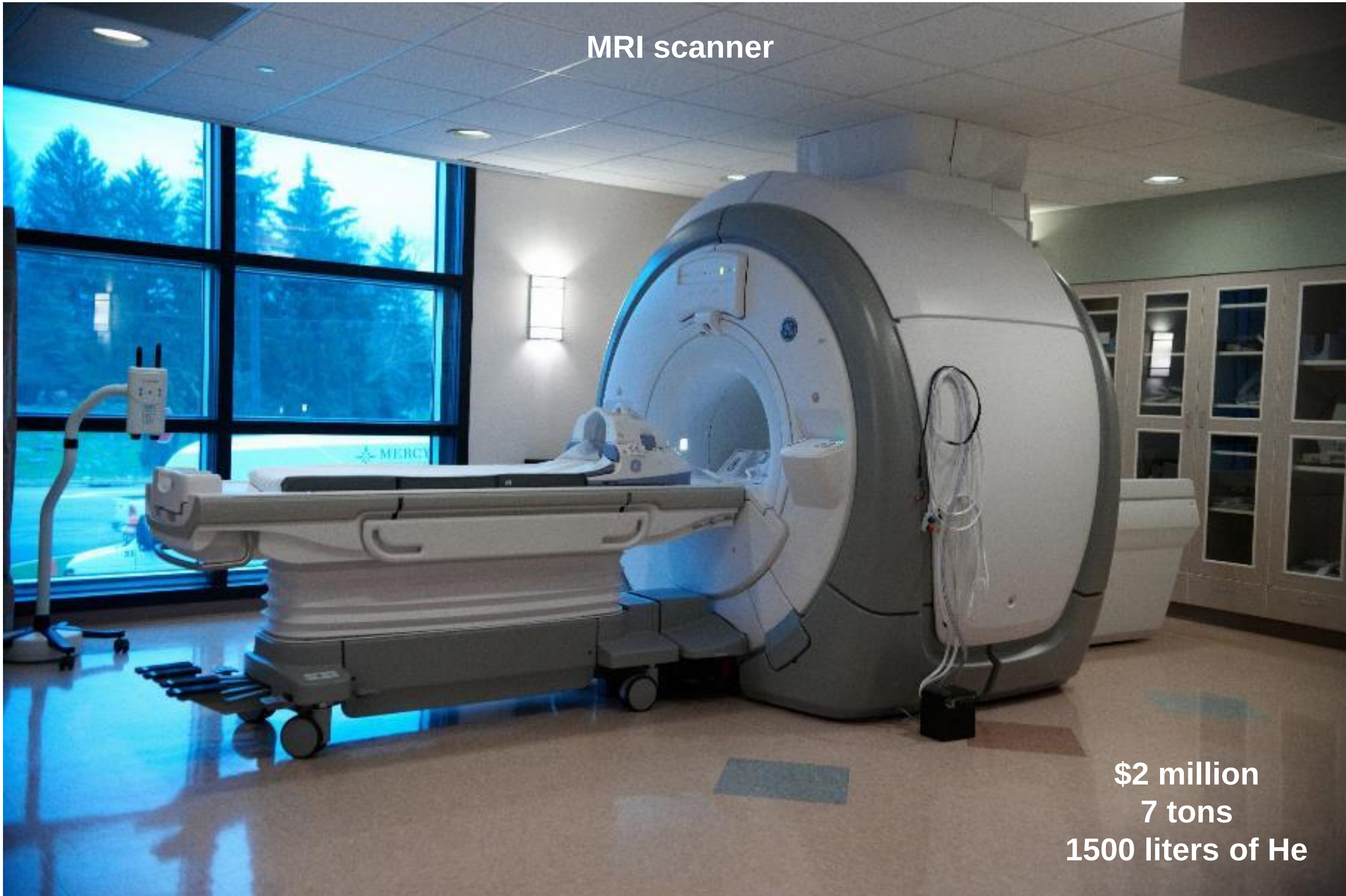
MRI scanner
$2 million
7 tons
1500 liters of He

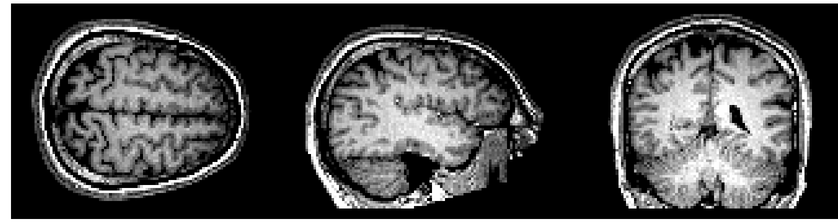

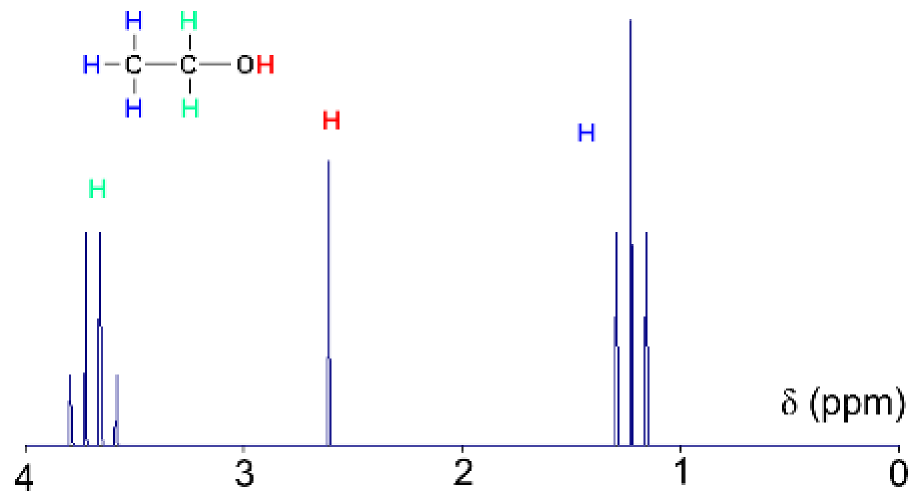
H H
H–C–C–OH
H H
H
H
H
δ (ppm)
4
3
2
1
0

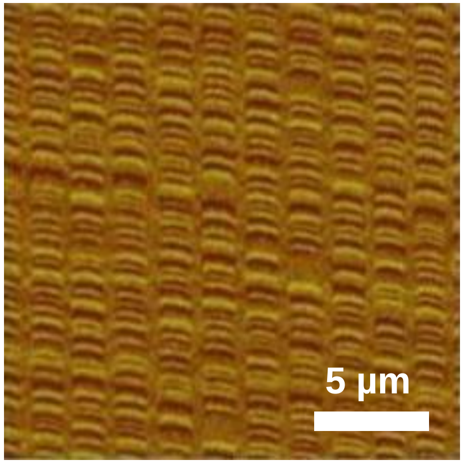

magnetic force microscopy (MFM)
image of hard drive surface

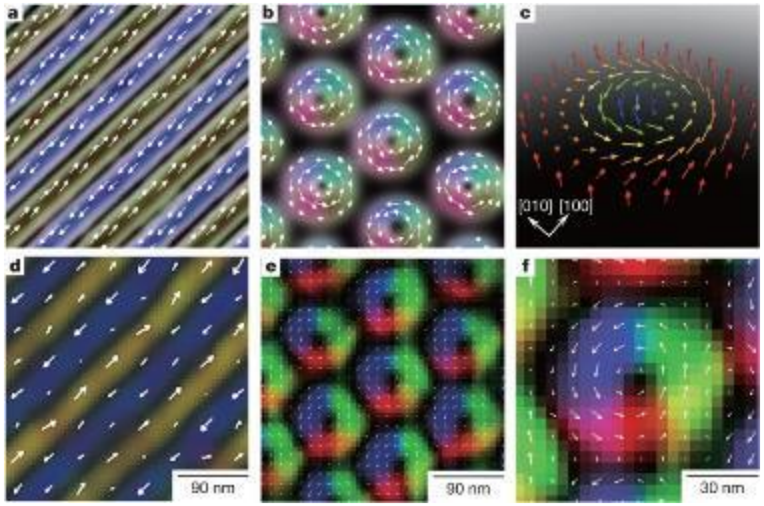

topological spin texture in helical magnet $Fe_{0.5}Co_{0.5}Si$
[Nature 465, 901 (2010)]

Magnetic sensors

sensitivity **resolution**

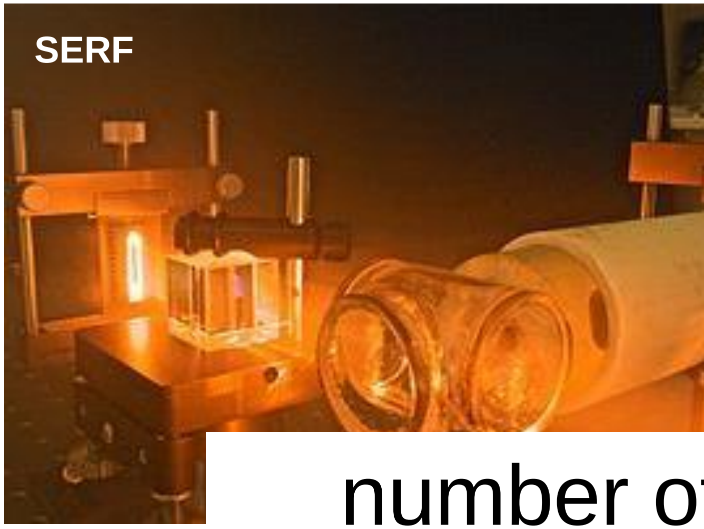

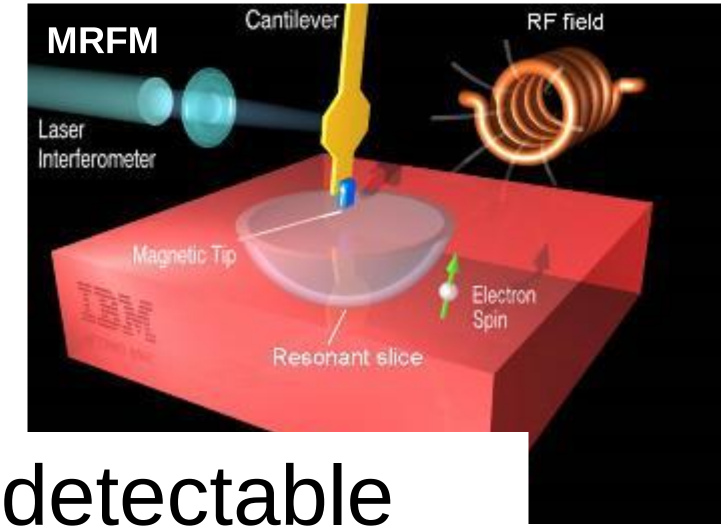

number of detectable magnetic moments (spins)

, 1560 (1994)

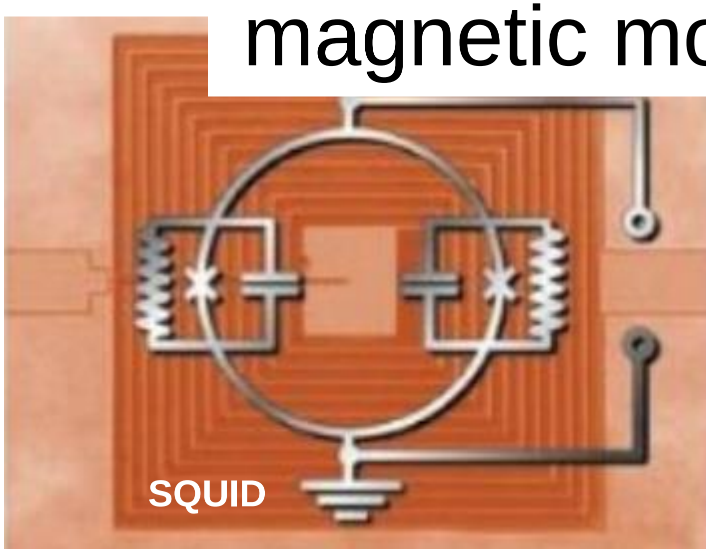

Phys.Rev.Lett. 12, 159 (1964)

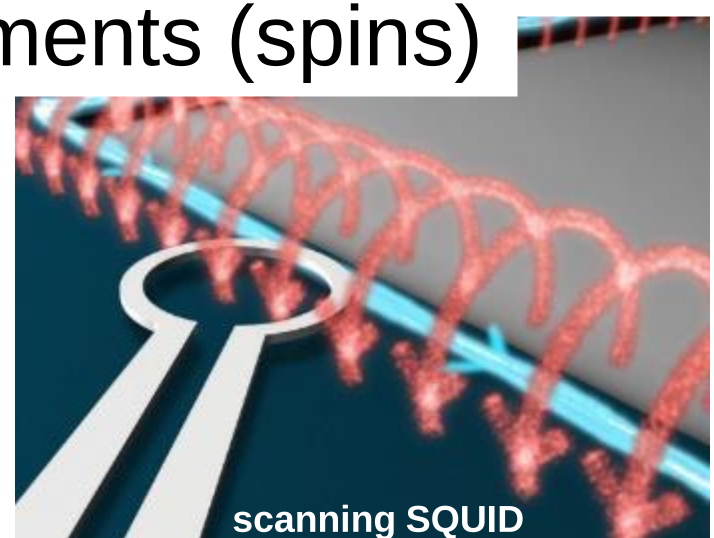

Appl.Phys.Lett. 61, 598 (1992)

The challenge: detecting a single proton spin

the ultimate limit of magnetization sensitivity

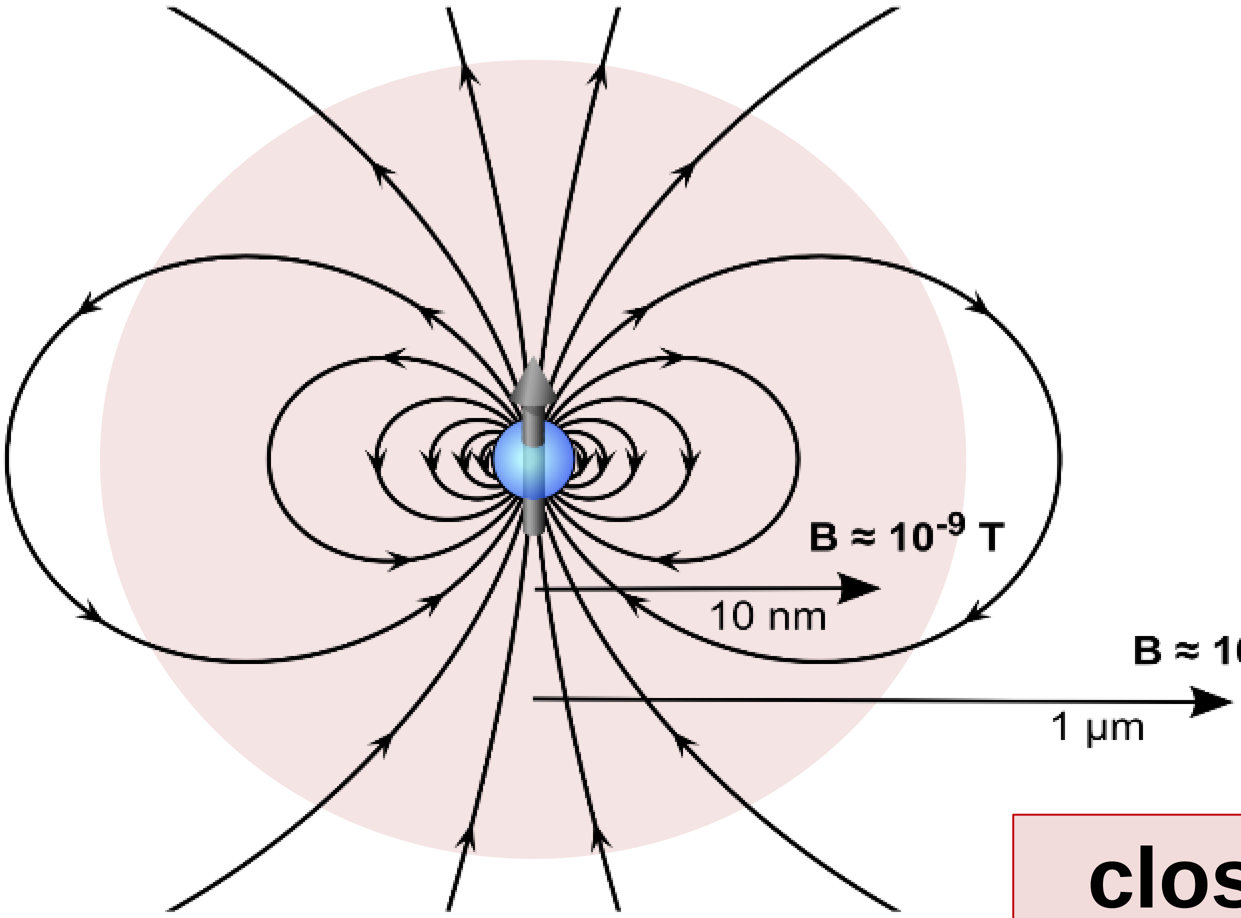

$$B_n \approx \mu_n / r^3$$

closer is better

Taking magnetic sensing to the nanoscale

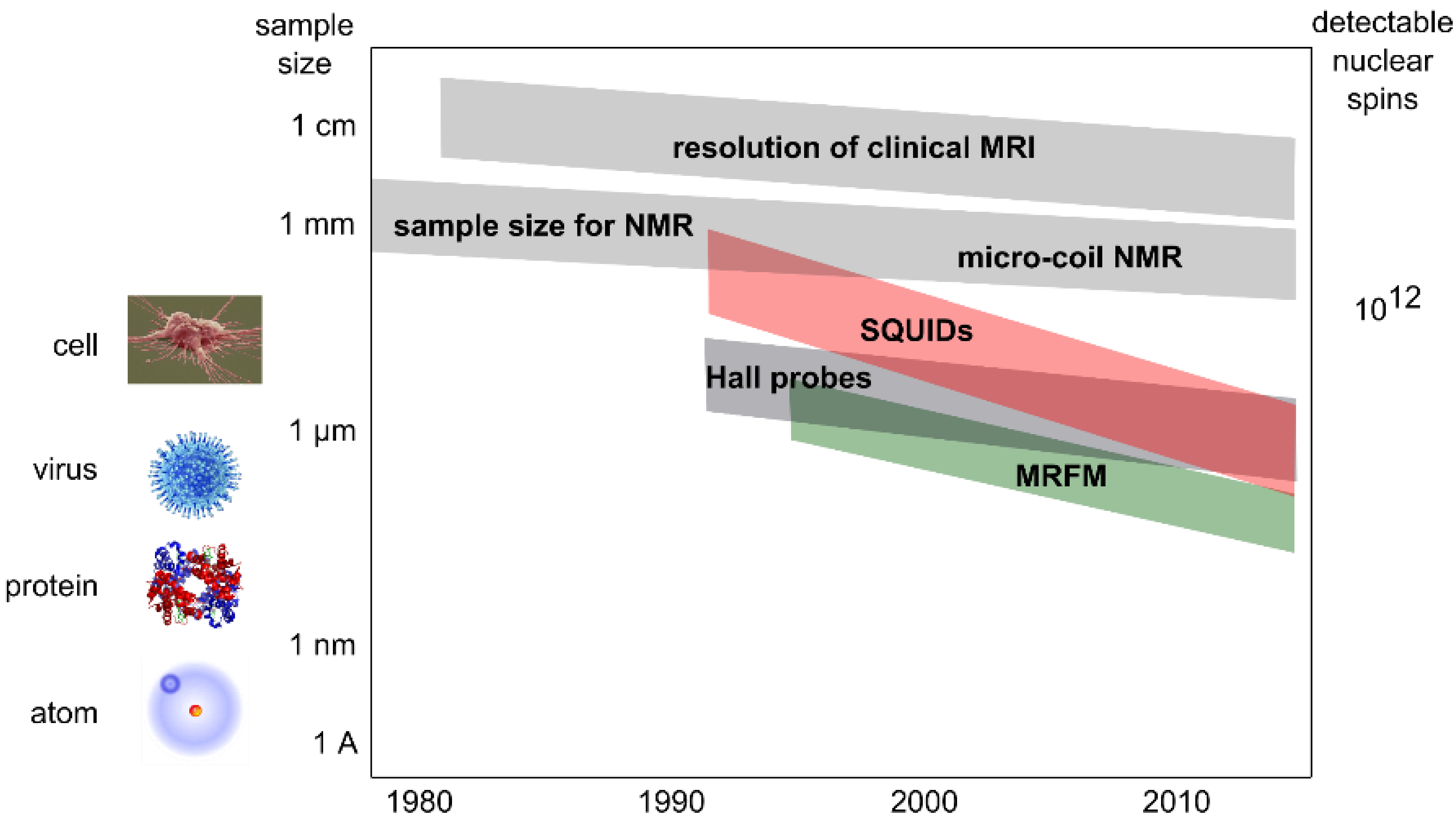

Taking magnetic sensing to the nanoscale

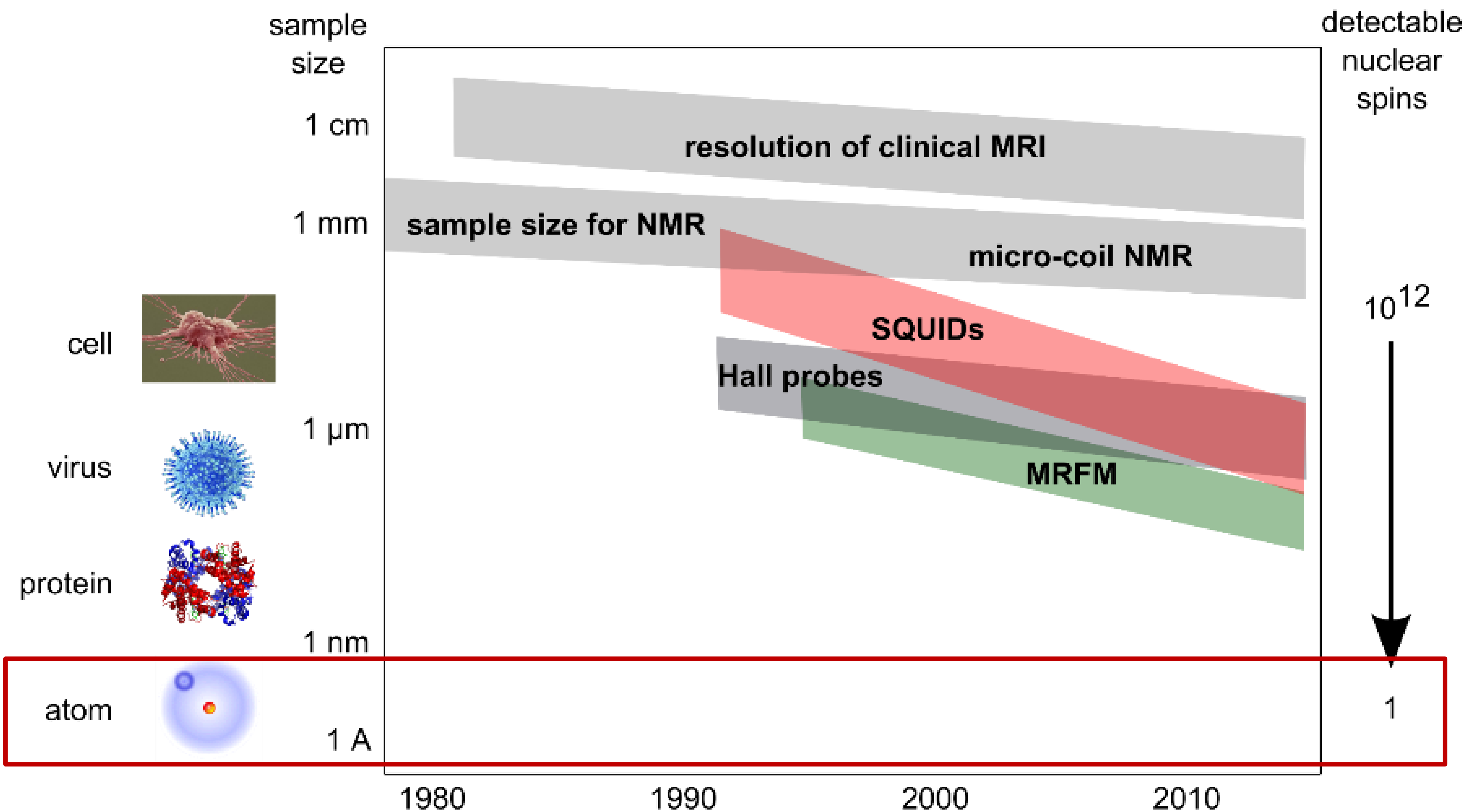

Taking magnetic sensing to the nanoscale

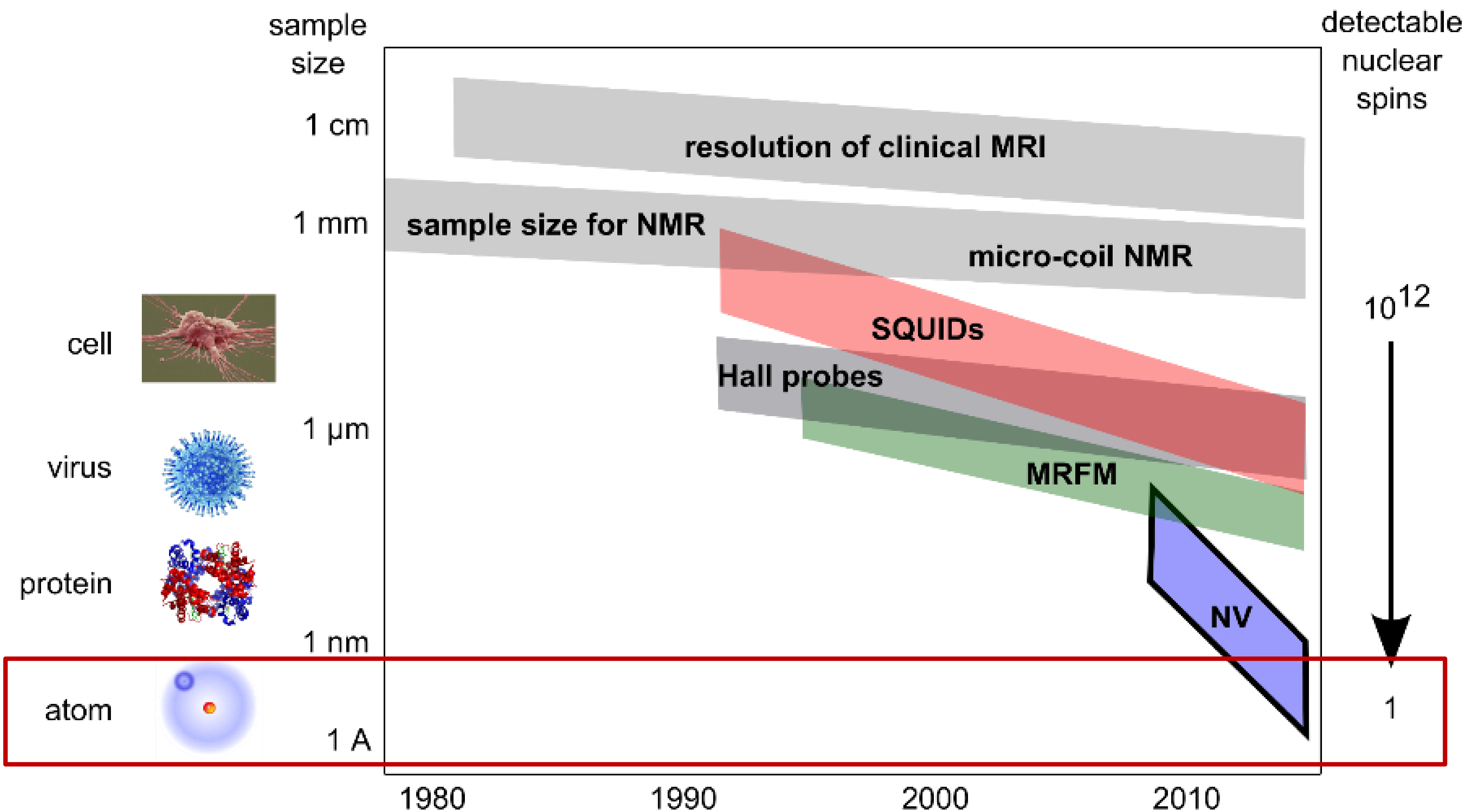

Outline

1. **The NV color center in diamond: introduction and applications**

2. Magnetic sensing with an NV center: the tools

3. NMR experiments with liquid hydrocarbons: detecting 10^4 nuclear spins →

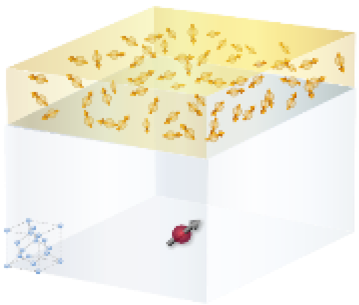

4. NMR spectroscopy of single protein molecules: detecting 400 nuclear spins →

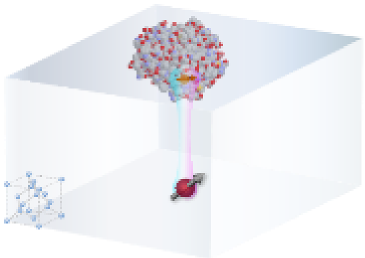

5. NMR with single nuclear spin sensitivity →

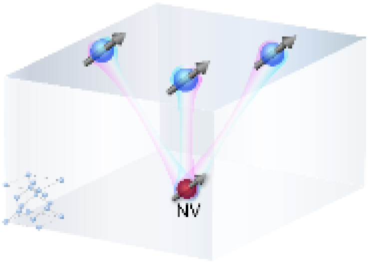

6. Outlook

Nitrogen-vacancy (NV) centers in diamond

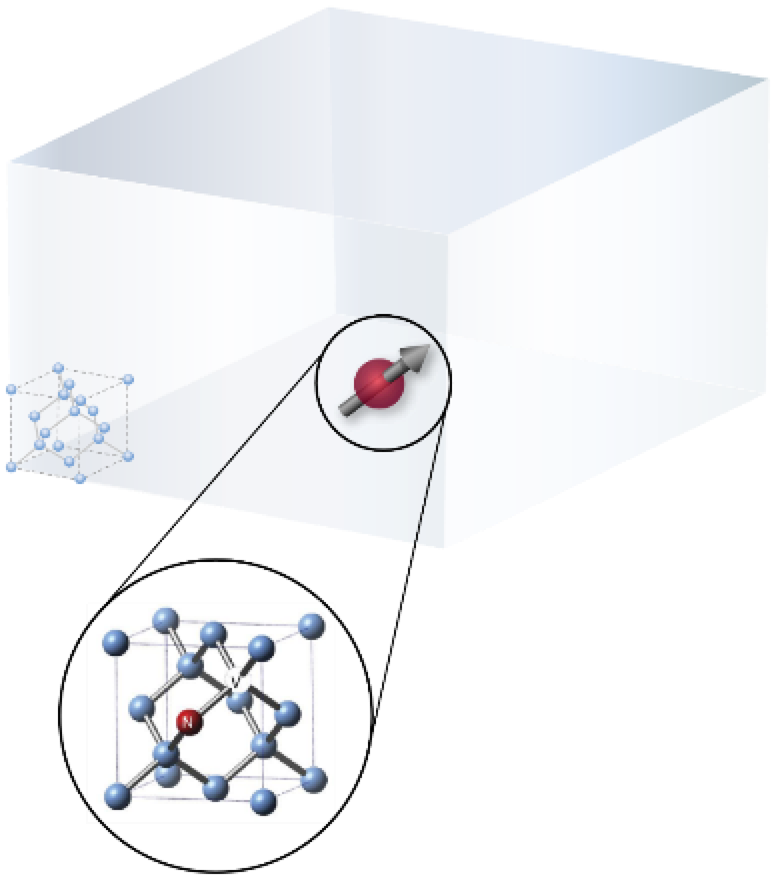

Nitrogen impurity next to a vacancy inside the diamond lattice

behaves like a single atom trapped inside the transparent diamond crystal

Making NV centers in diamond

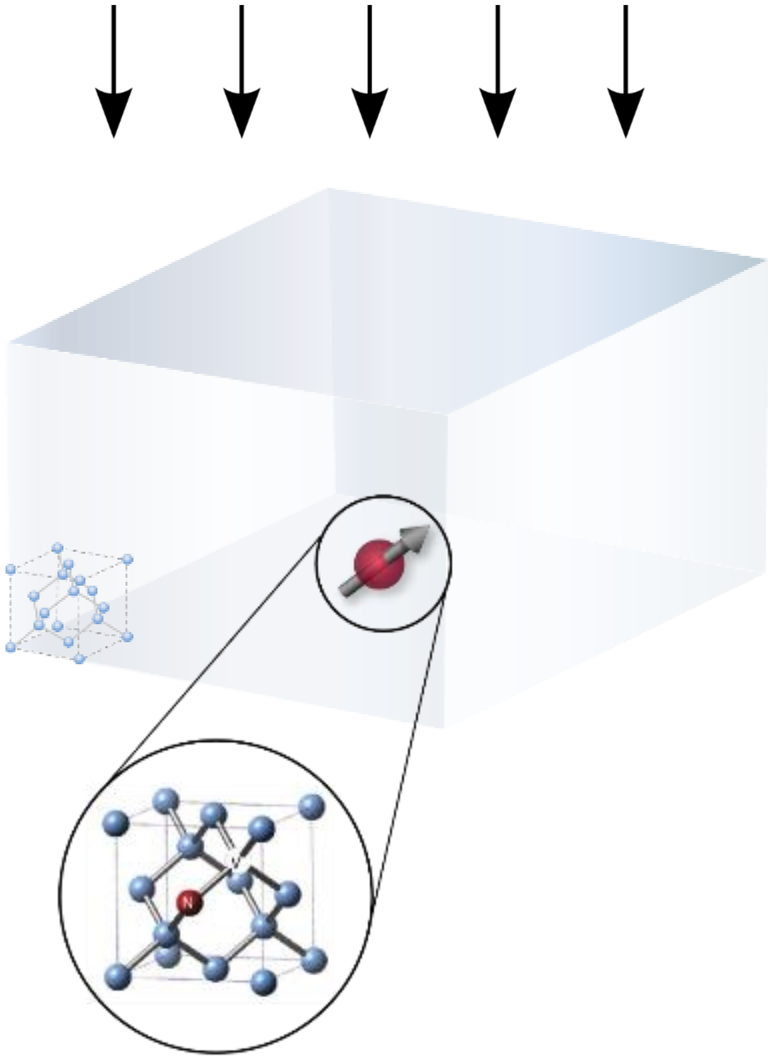

1. “electronic-grade” diamond crystal
2. nitrogen ion implantation
3. anneal at 800 C

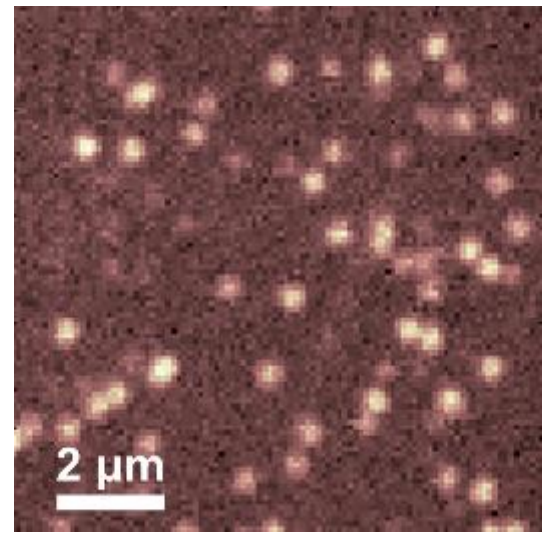

behaves like a single atom trapped inside the transparent diamond crystal

Properties of NV centers in diamond

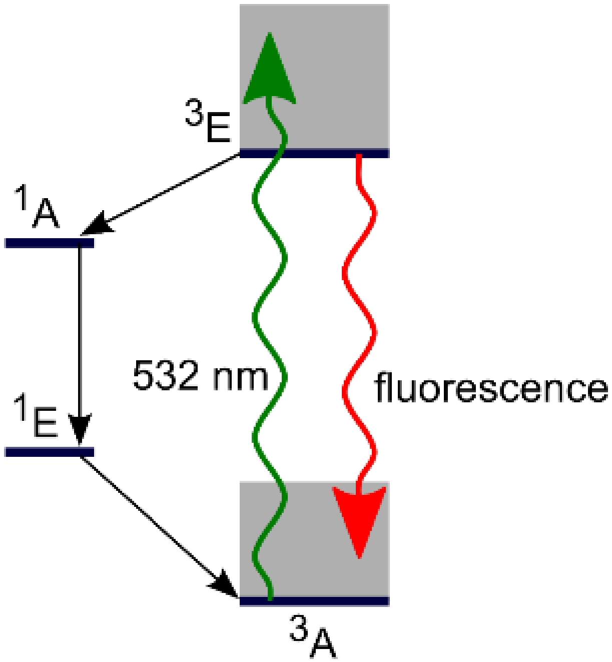

1. the relevant levels of the NV center are within diamond bandgap, an electric-dipole transition

Properties of NV centers in diamond

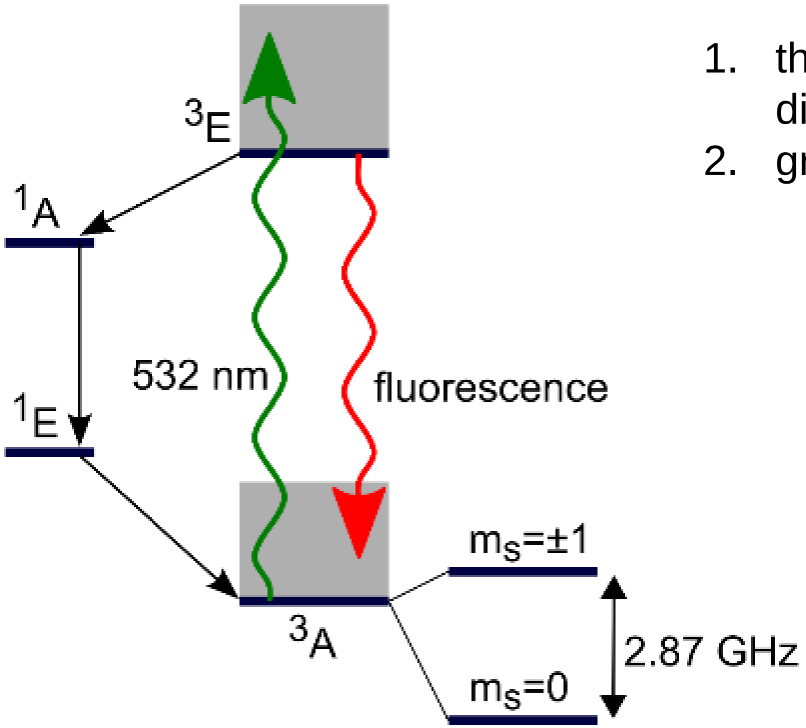

1. the relevant levels of the NV center are within diamond bandgap, an electric-dipole transition
2. ground-state electron spin S=1

Properties of NV centers in diamond

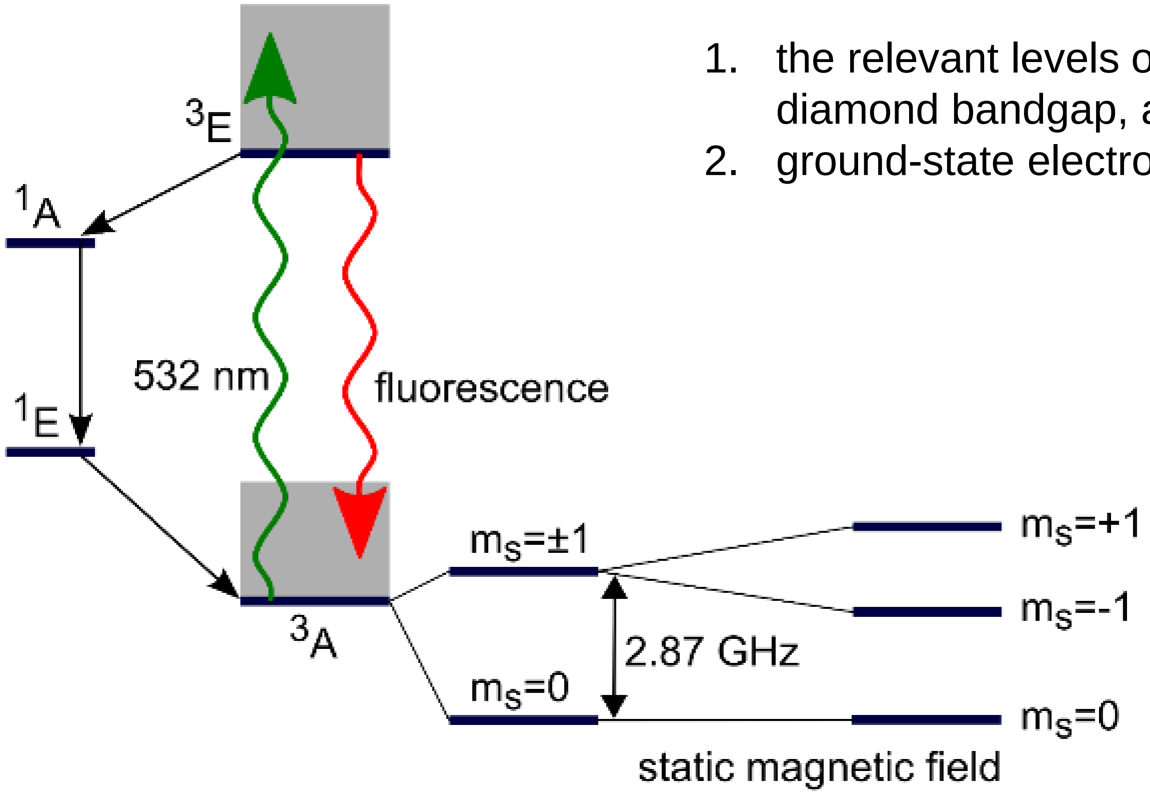

1. the relevant levels of the NV center are within diamond bandgap, an electric-dipole transition
2. ground-state electron spin S=1

Properties of NV centers in diamond

1. the relevant levels of the NV center are within diamond bandgap, an electric-dipole transition
2. ground-state electron spin S=1

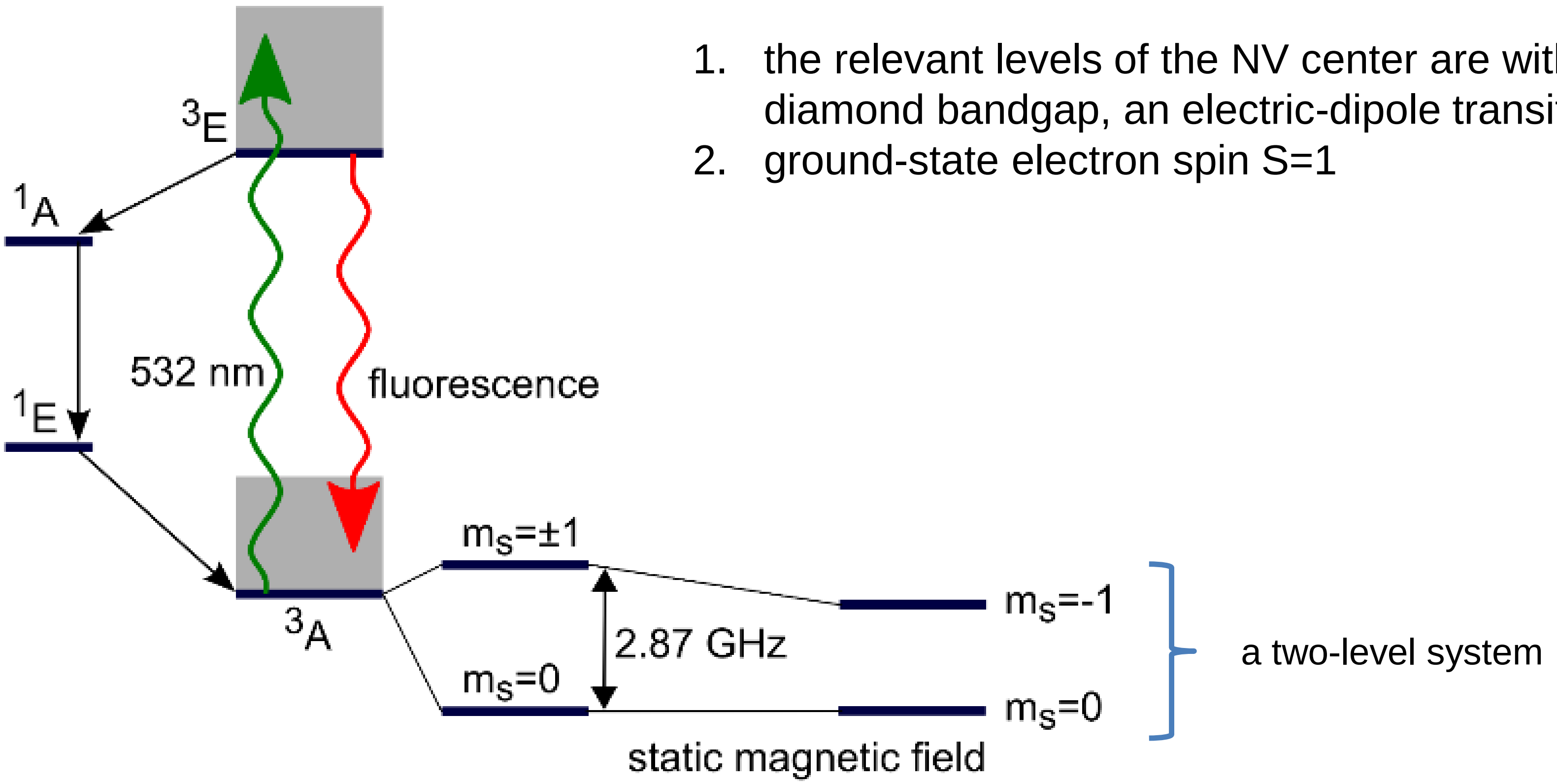

A schematic sensing experiment with an NV center

1. the relevant levels of the NV center are within diamond bandgap, an electric-dipole transition
2. ground-state electron spin S=1

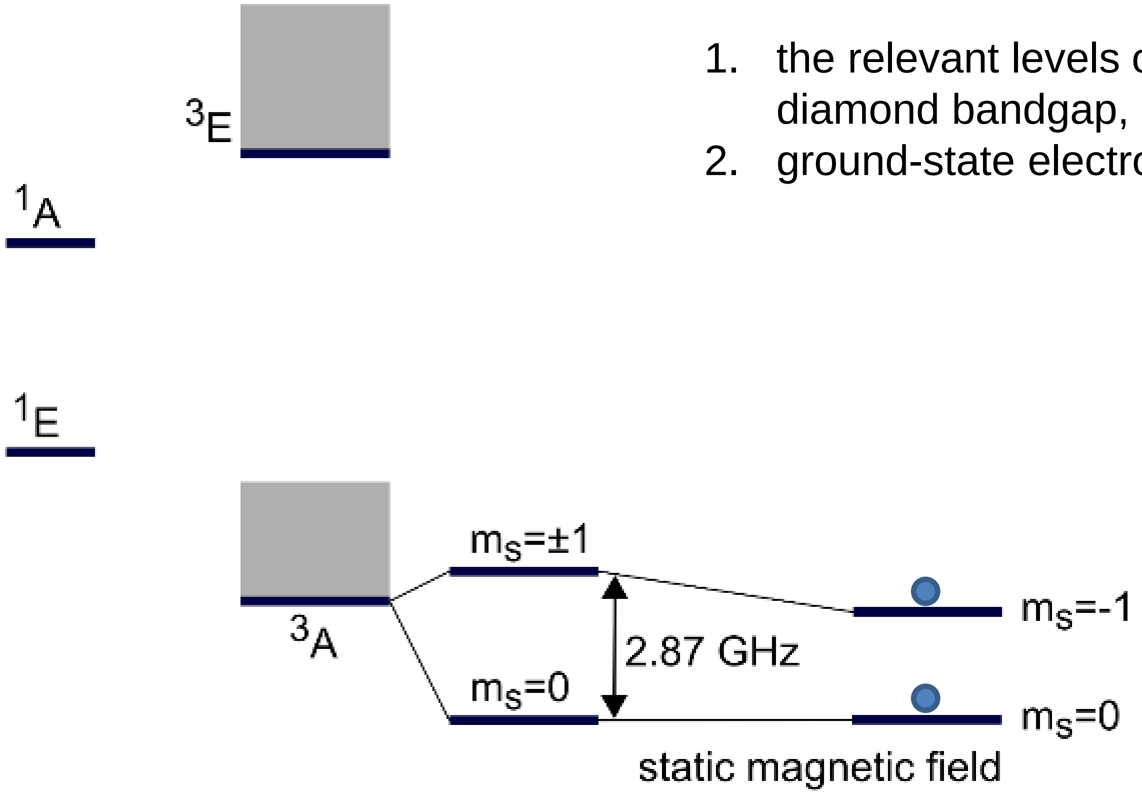

equal populations at room temperature

A schematic sensing experiment with an NV center

1. the relevant levels of the NV center are within diamond bandgap, an electric-dipole transition
2. ground-state electron spin S=1
3. **optical initialization of spin state**

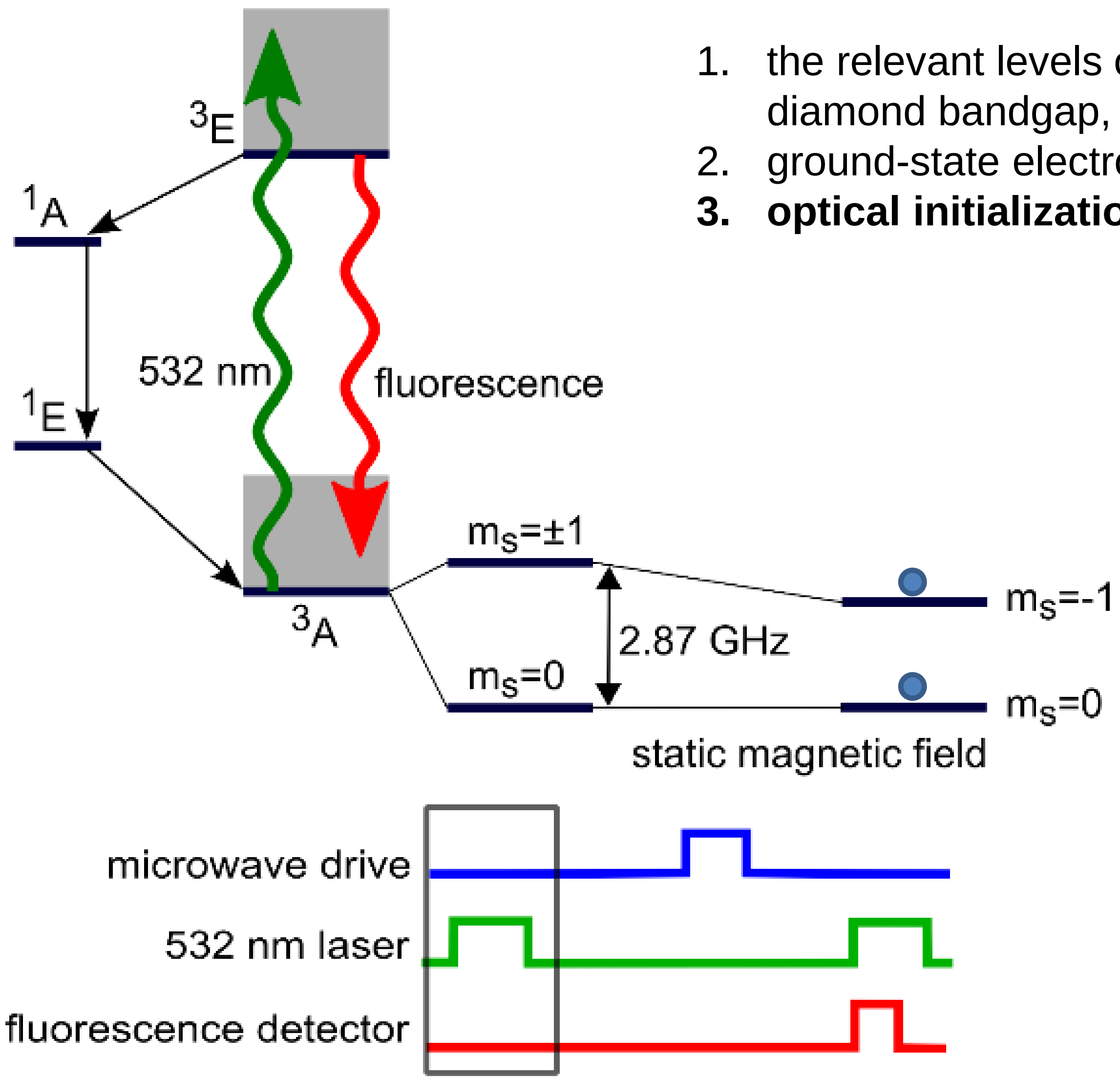

optical pumping

A schematic sensing experiment with an NV center

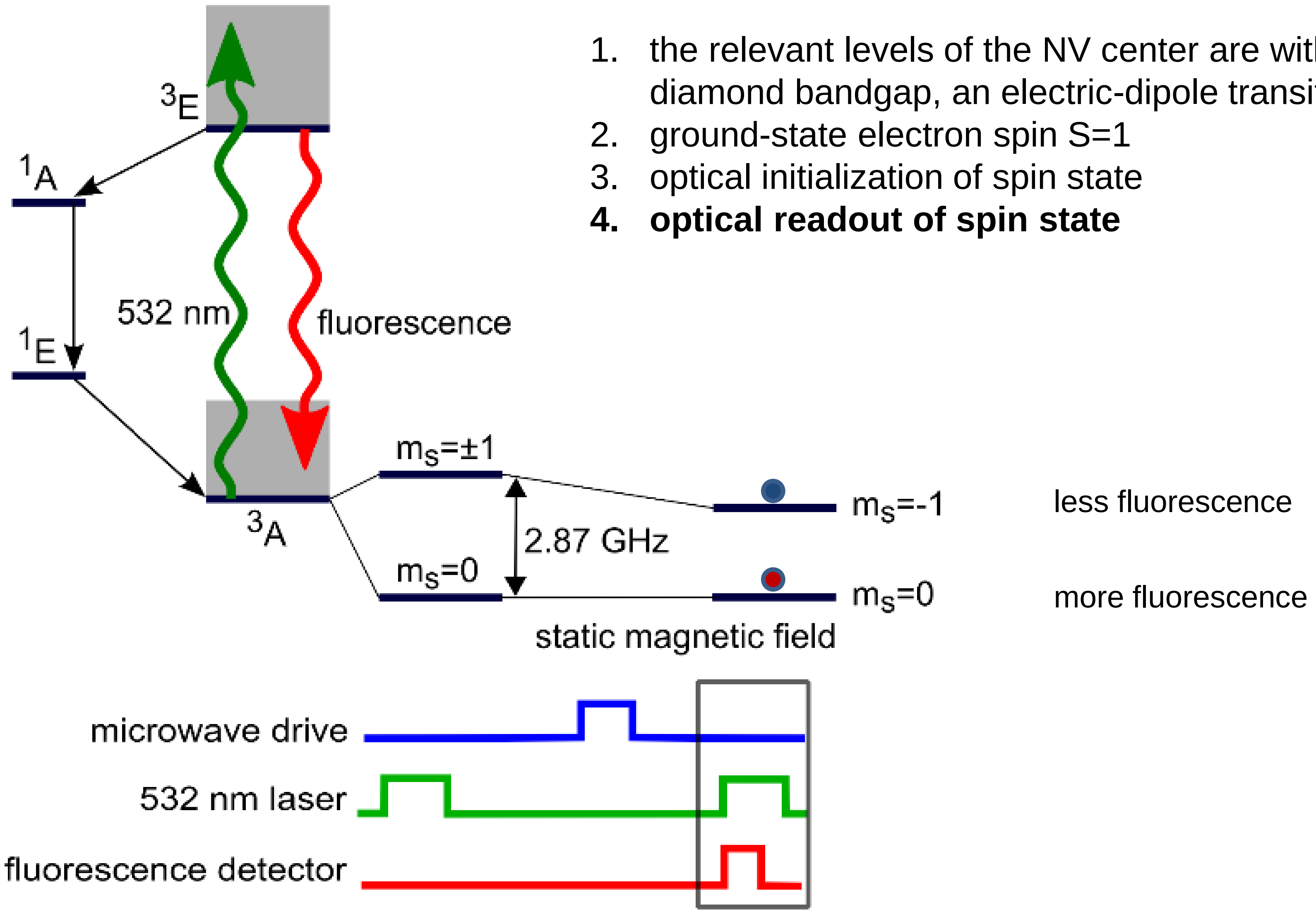

1. the relevant levels of the NV center are within diamond bandgap, an electric-dipole transition
2. ground-state electron spin S=1
3. optical initialization of spin state
4. **optical readout of spin state**

A schematic sensing experiment with an NV center

1. the relevant levels of the NV center are within diamond bandgap, an electric-dipole transition
2. ground-state electron spin S=1
3. optical initialization of spin state
4. optical readout of spin state
5. **microwave manipulation of spin state**

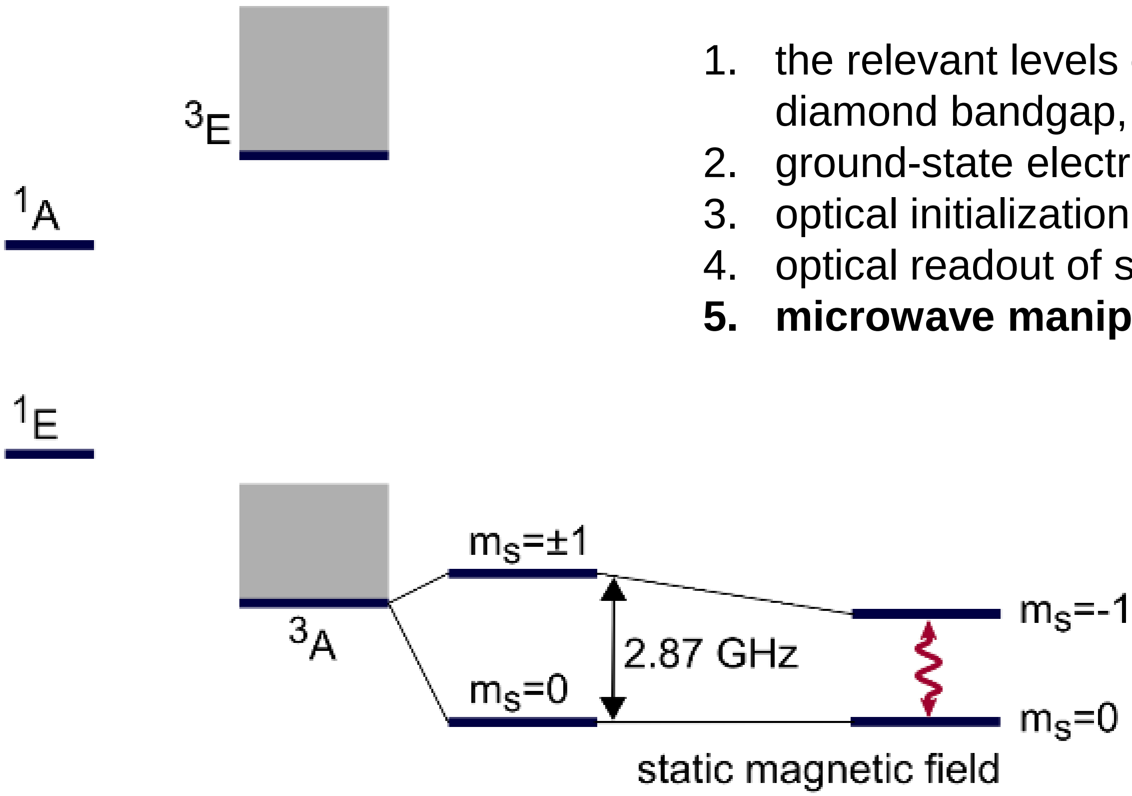

microwave drive

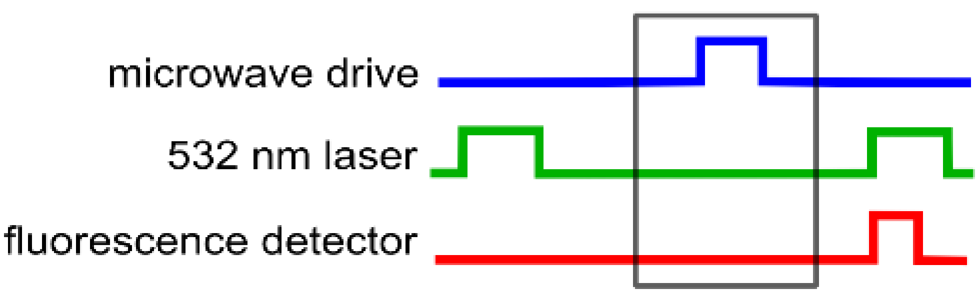

A schematic sensing experiment with an NV center

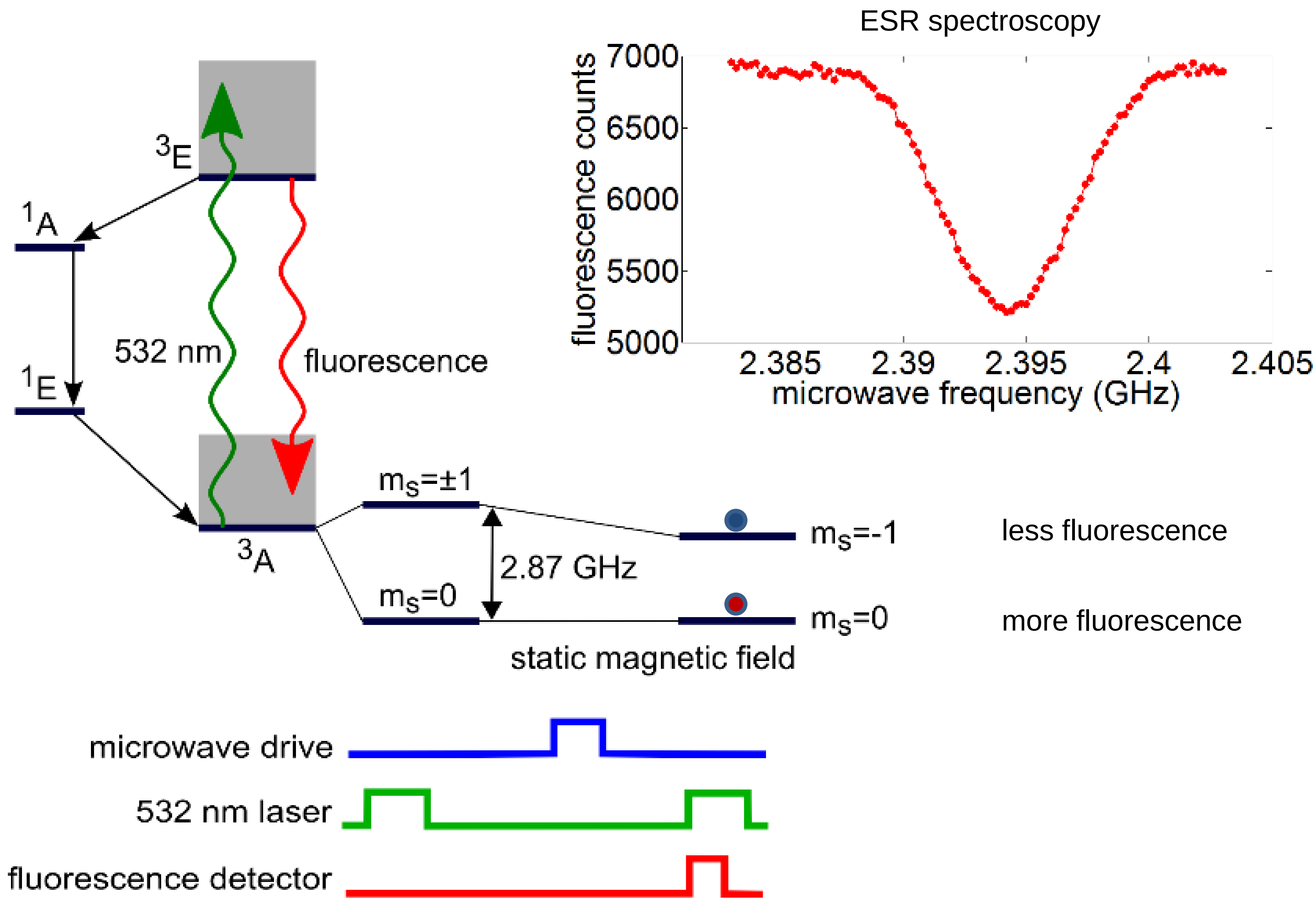

A schematic sensing experiment with an NV center

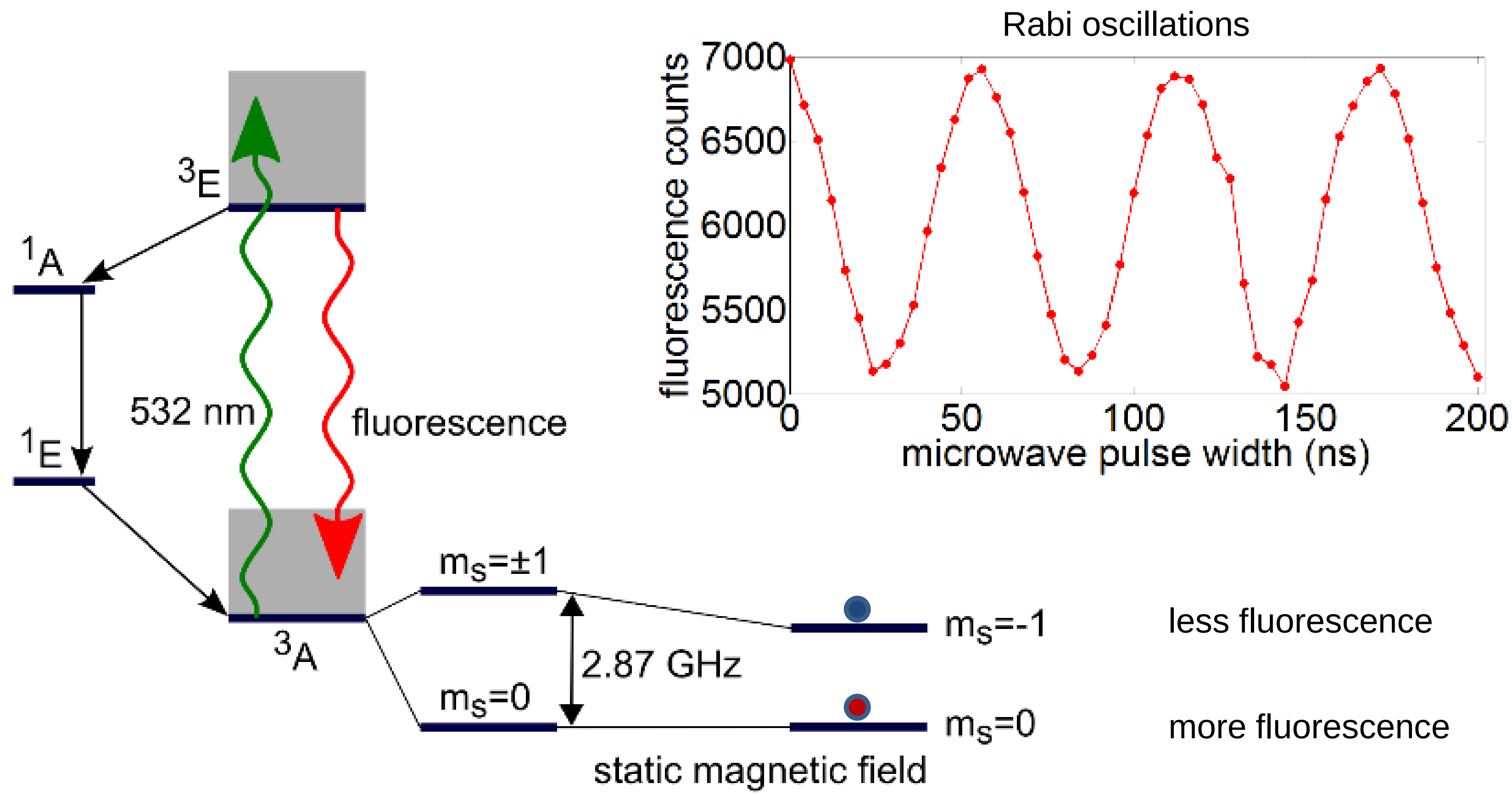

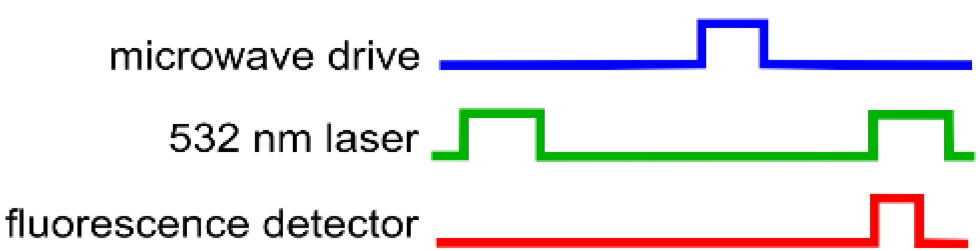

a room-temperature single-spin quantum system

Experimental apparatus

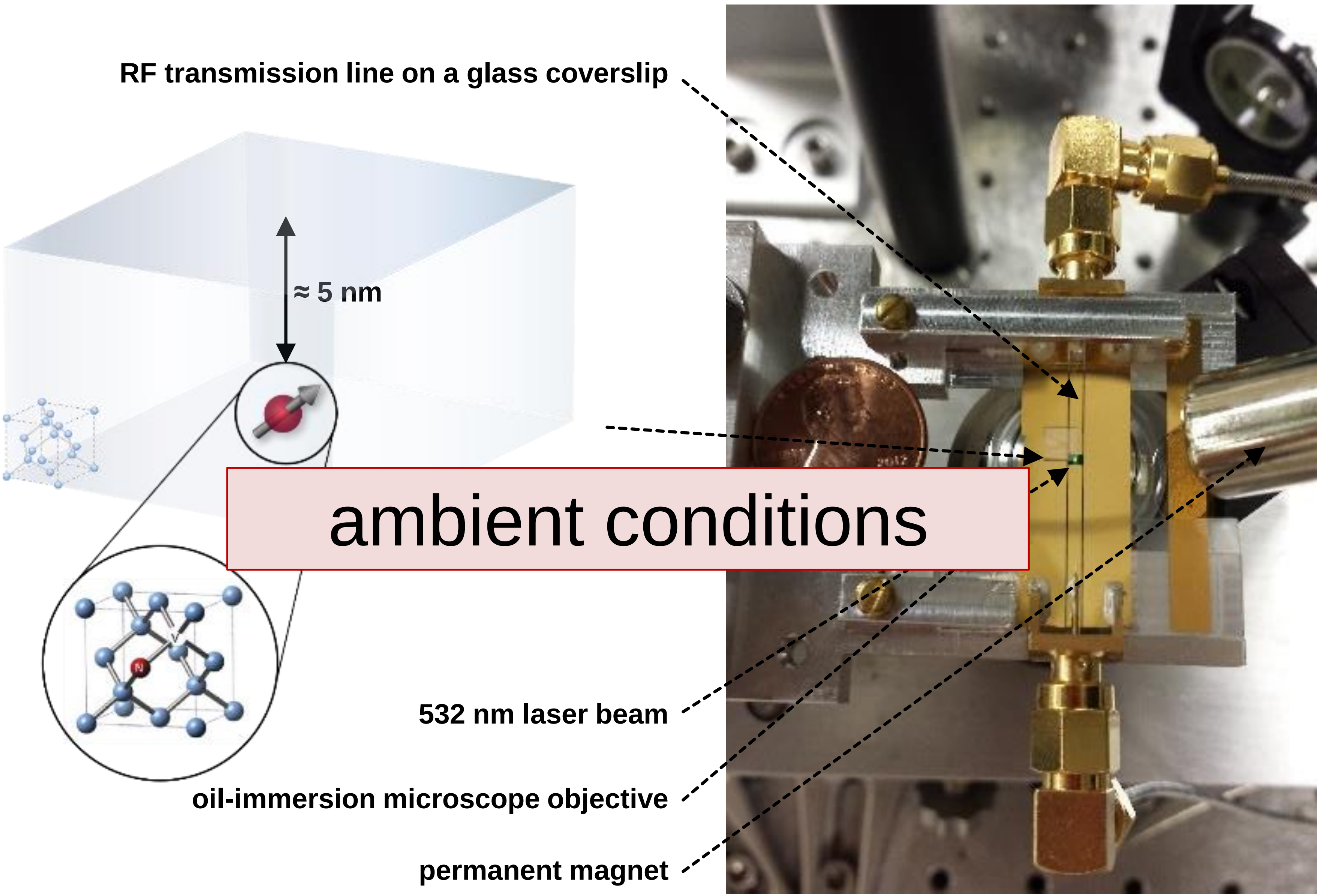

ambient conditions

Applications of NV centers

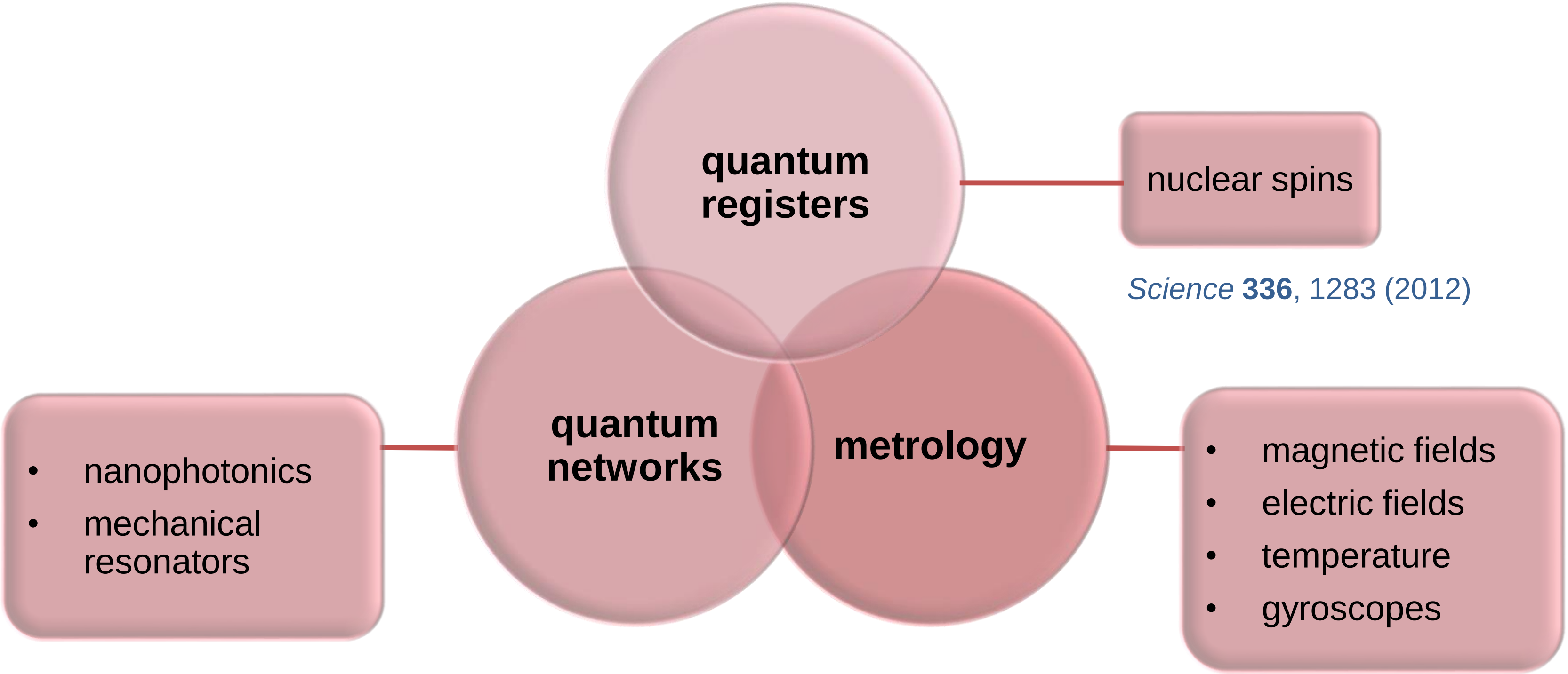

Science **336**, 1283 (2012)

Nature **466**, 730 (2010)
Nature **497**, 86 (2013)
Science **335**, 1603 (2012)

Nature Physics **4**, 810 (2008)
Science **339**, 561 (2013)
Nature Physics **7**, 459 (2011)
Nature **500**, 54 (2013)
Phys. Rev. A **86**, 0521226 (2012)

Physics Today **67**, 38 (2014)
Scientific American **297**, 84 (2007)

Outline

1. The NV color center in diamond: introduction and applications

2. Magnetic sensing with an NV center: the tools

3. NMR experiments with liquid hydrocarbons: detecting 10^4 nuclear spins

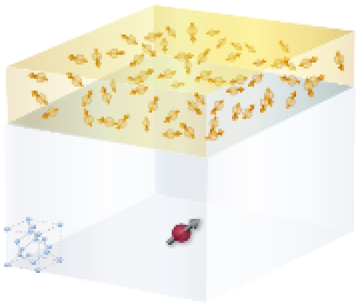

4. NMR spectroscopy of single protein molecules: detecting 400 nuclear spins

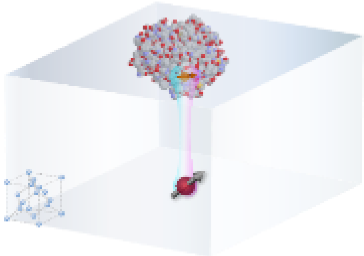

5. NMR with single nuclear spin sensitivity

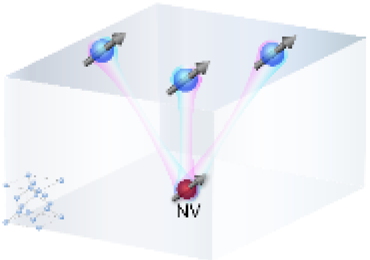

6. Outlook

NV-based magnetic sensing schemes

population and coherence of ground-state sublevels

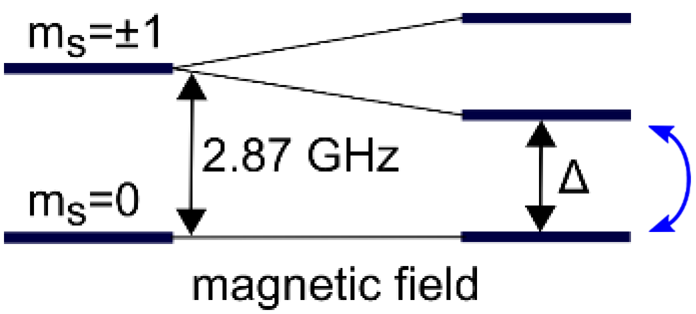

- **fast-oscillating fields (>GHz) → NV population transfer (incoherent)**

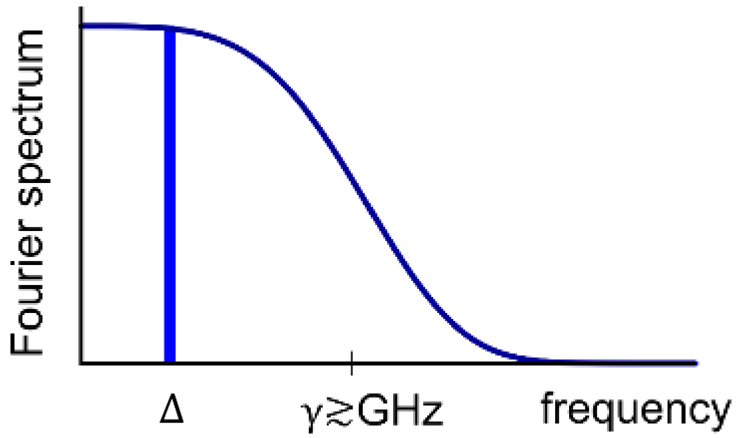

all-optical magnetic detection of single-atom Gd spins at room temperature

Alex Sushkov, Nick Chisholm, Igor Lovchinsky, et al., *Nano Lett*. **14**, 6443 (2014)

probing magnetic Johnson noise at the nanometer scale, electron ballistic transport

Shimon Kolkowitz, Arthur Safira, et al., *Science,* in press

NV-based magnetic sensing schemes

population and coherence of ground-state sublevels

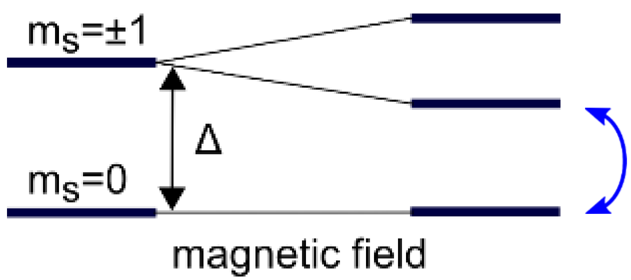

- fast-oscillating fields (>GHz) → NV population transfer (incoherent)
- **radiofrequency fields (kHz – 100 MHz) → NV echo magnetometry (coherent)**

Larmor precession of a nuclear spin:

NV spin echo magnetic sensing

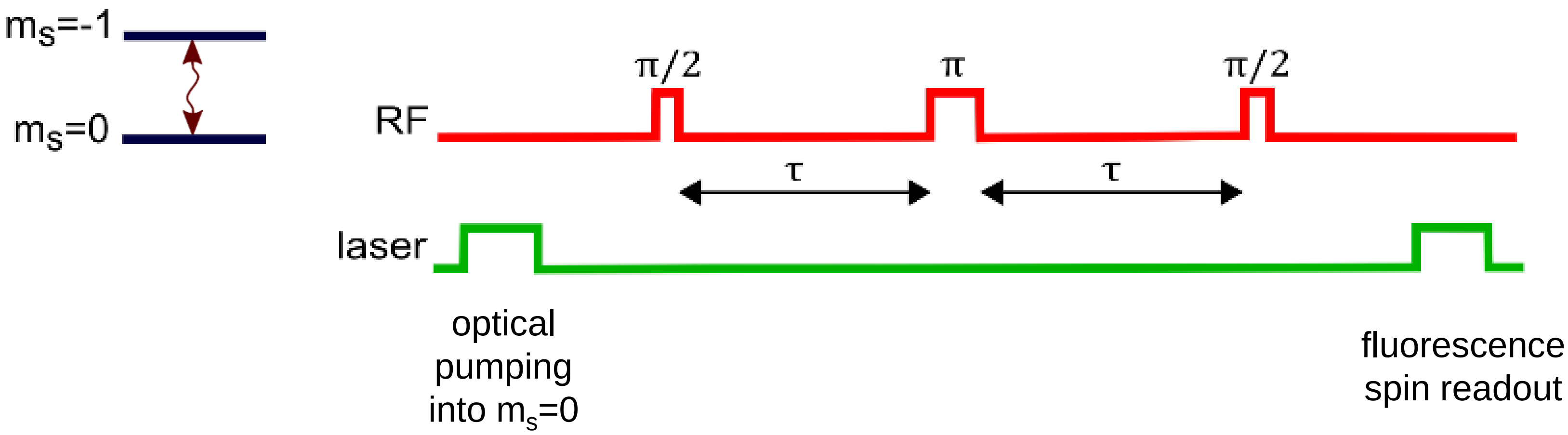

NV spin echo magnetic sensing

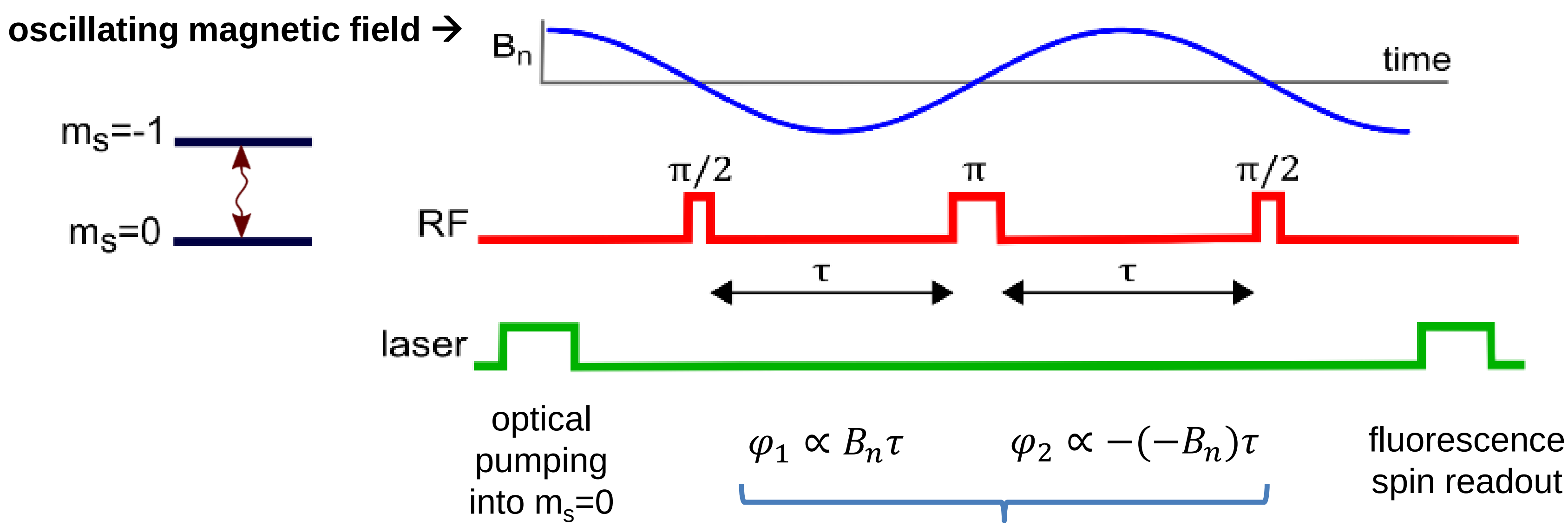

$$\varphi_1 + \varphi_2 \propto 2B_n\tau$$

spin echo sensitive to magnetic fields at frequencies $\sim 1/2\tau$

NV CPMG (Carr-Purcell-Meiboom-Gill) magnetic sensing

NV center spin → magnetic spectrometer

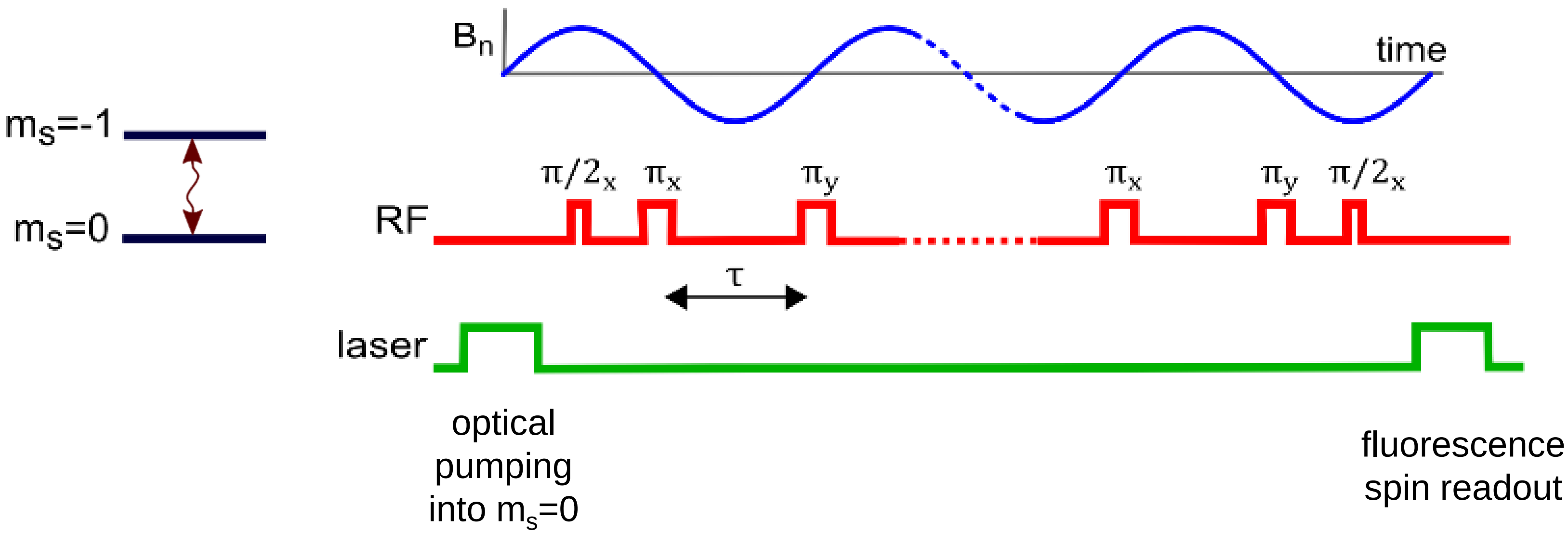

- robust against pulse errors
- longer NV T_2 due to dynamical decoupling from environment
- spectral selectivity by varying free evolution interval τ

Outline

1. The NV color center in diamond: introduction and applications

2. Magnetic sensing with an NV center: the tools

3. **NMR experiments with liquid hydrocarbons: detecting 10^4 nuclear spins** →

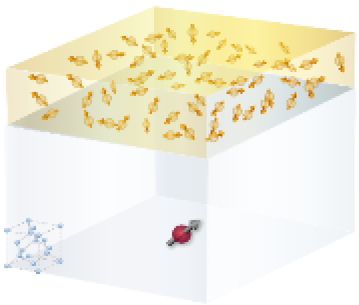

4. NMR spectroscopy of single protein molecules: detecting 400 nuclear spins →

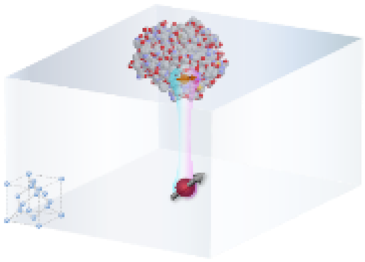

5. NMR with single nuclear spin sensitivity →

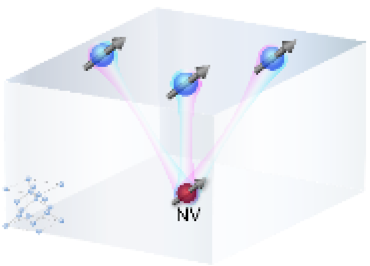

6. Outlook

An NV-based NMR experiment

target sample with nuclear spins

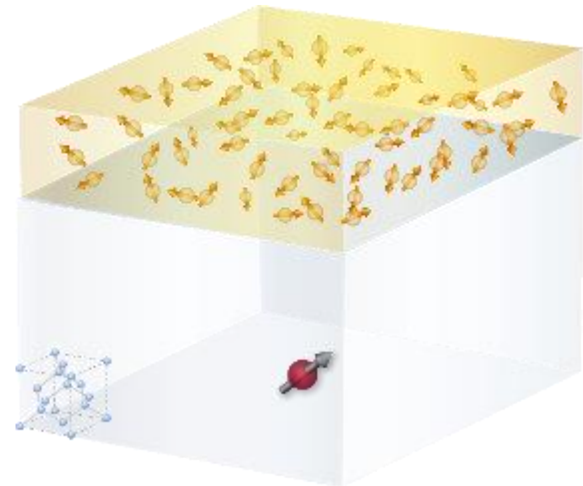

randomly-oriented proton spins add to give zero net magnetic field:

$$\langle B_n \rangle = 0$$

but there is a "statistical polarization" $\sim\sqrt{N}$

$$\boxed{\langle B_n^2 \rangle \neq 0}$$

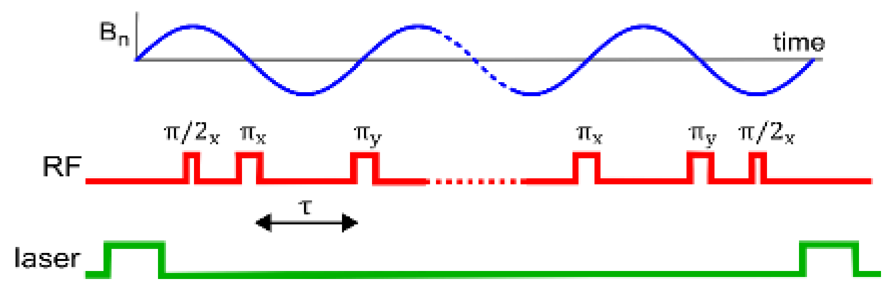

measure variance of nuclear magnetic field: $\langle B_n^2 \rangle$

First NMR experiments: protons in immersion oil

NV magnetometry measures magnetic field B_n from proton spins in objective oil

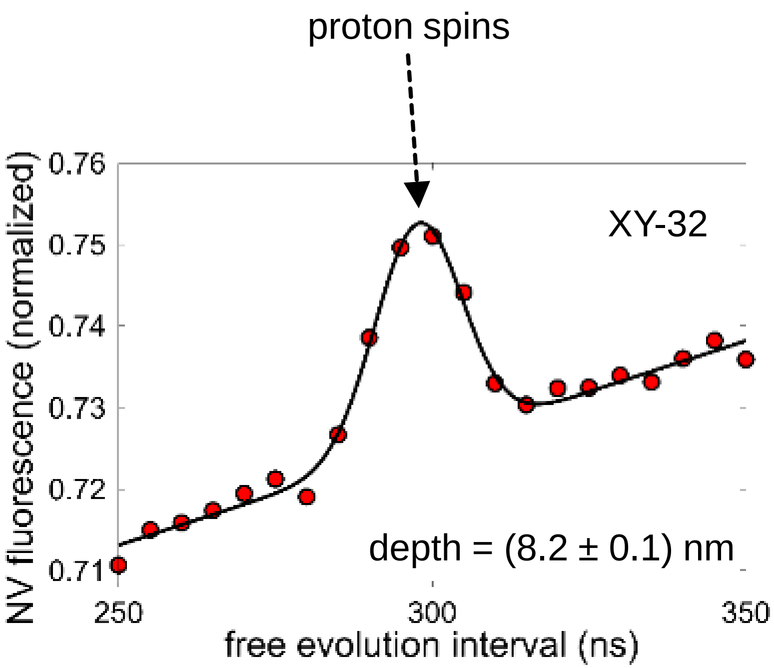

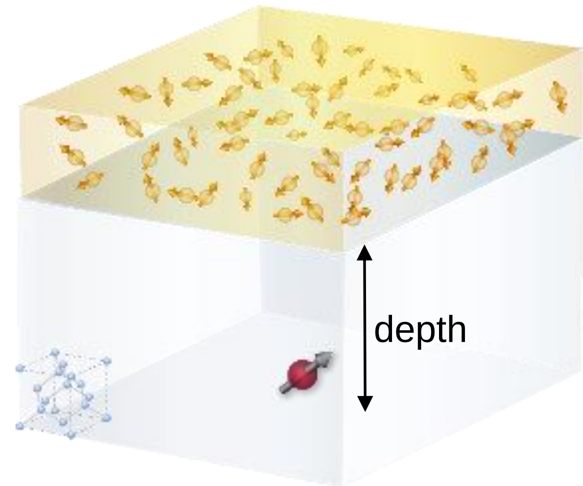

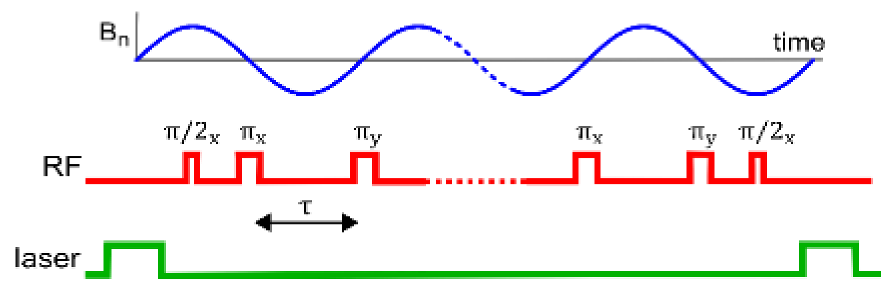

detecting ≈10^4 nuclear spins

NV depth extracted from proton peak magnitude

S. DeVience, L.Pham, I. Lovchinsky, et al., *Nature Nano*, DOI: 10.1038 (2015)

H. Mamin, et al., *Science* **339**, 557 (2013)
T. Staudacher et al., *Science* **339**, 561 (2013)

Outline

1. The NV color center in diamond: introduction and applications

2. Magnetic sensing with an NV center: the tools

3. NMR experiments with liquid hydrocarbons: detecting 10^4 nuclear spins

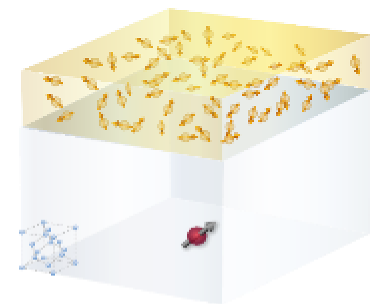

4. **NMR spectroscopy of single protein molecules: detecting 400 nuclear spins**

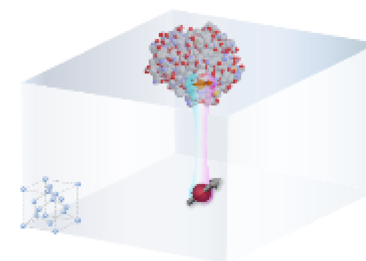

5. NMR with single nuclear spin sensitivity

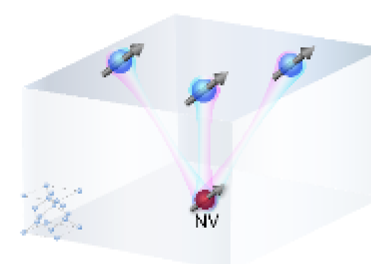

6. Outlook

Experimental sensitivity parameters

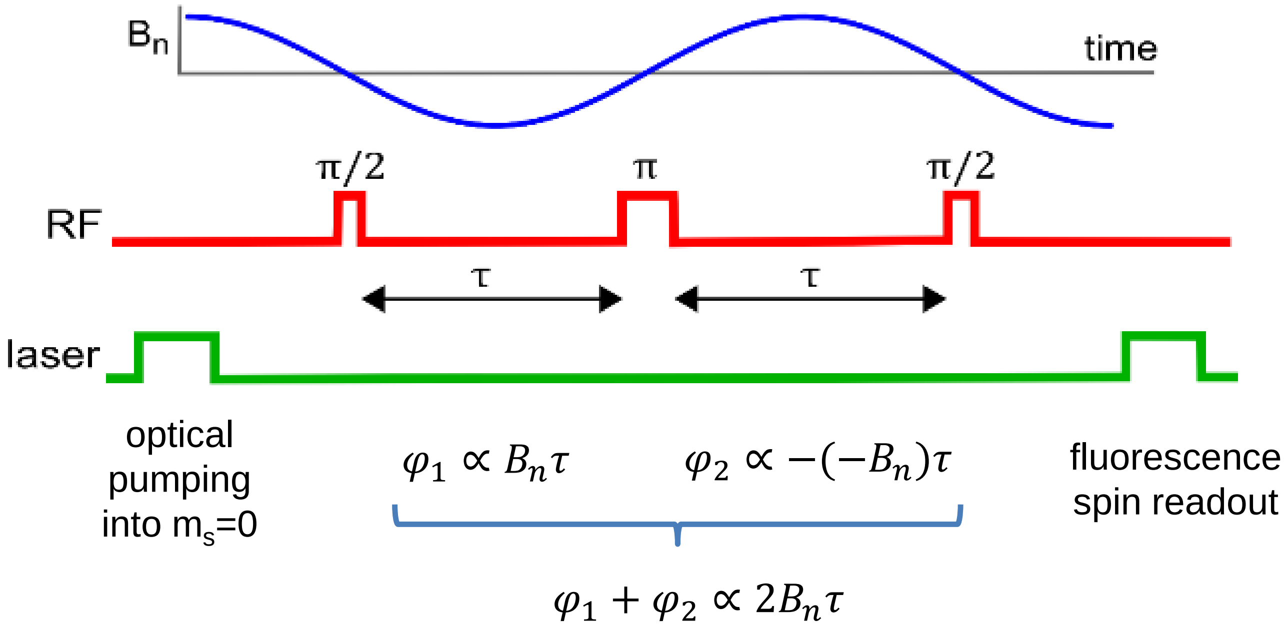

signal: $\langle B_n^2 \rangle \approx \mu_n^2 / r^6$ ◄------- closer is better

NV spin coherence time: $2\tau \approx T_2$ ◄--------------- longer T_2 is better

NV spin readout fidelity ◄-------------------------- higher fidelity is better

Coherence times of shallow NV centers

shallow NV centers display faster decoherence

likely due to surface electron spins (dangling bonds)

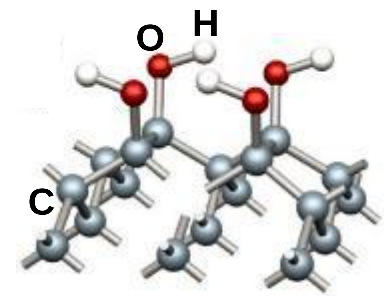

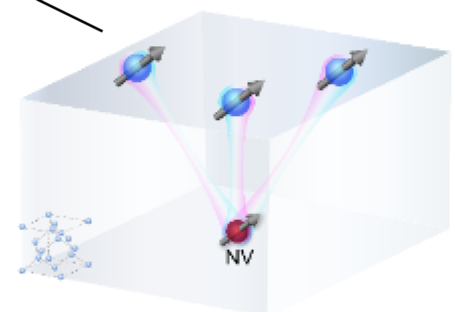

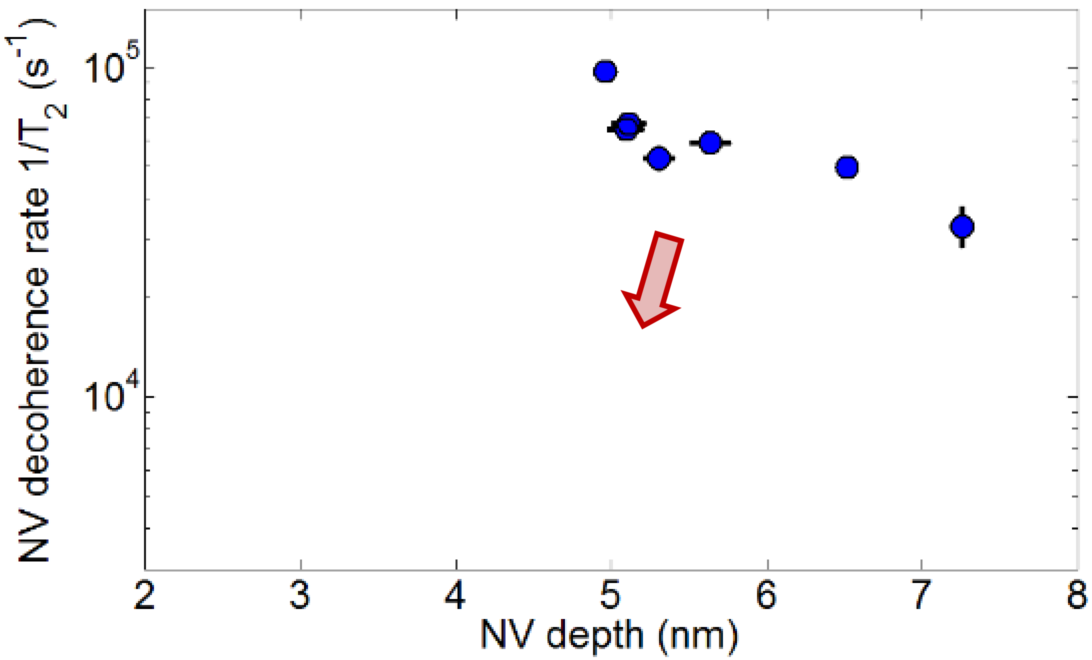

anneal diamond at 465 C in oxygen atmosphere

10-fold improvement in T_2

Igor Lovchinsky, Alex Sushkov, Elana Urbach, Nathalie de Leon, et al.
manuscript in preparation

NV spin readout

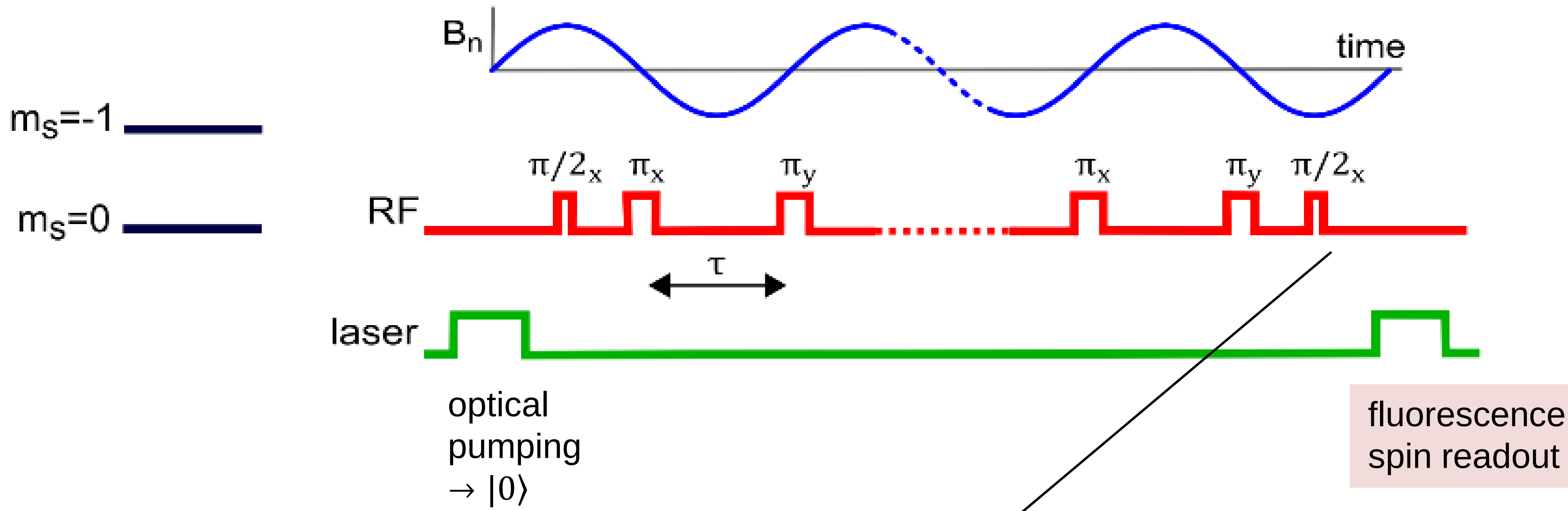

measurement result is stored in the NV electron spin state:

$$\alpha|0\rangle + \beta|-1\rangle$$

optical readout destroys NV electron spin state $\rightarrow |0\rangle$

how well did we measure α, β?

< 1% fidelity → poor fluorescence collection efficiency

Improving NV spin readout using quantum logic

electron J=1 $\qquad$ ^{15}N nuclear I=1/2

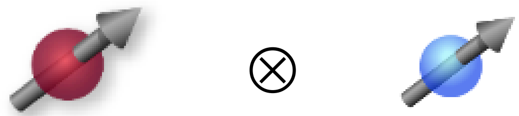

hyperfine: $H = A\boldsymbol{J}\cdot\boldsymbol{I}$

electron spin

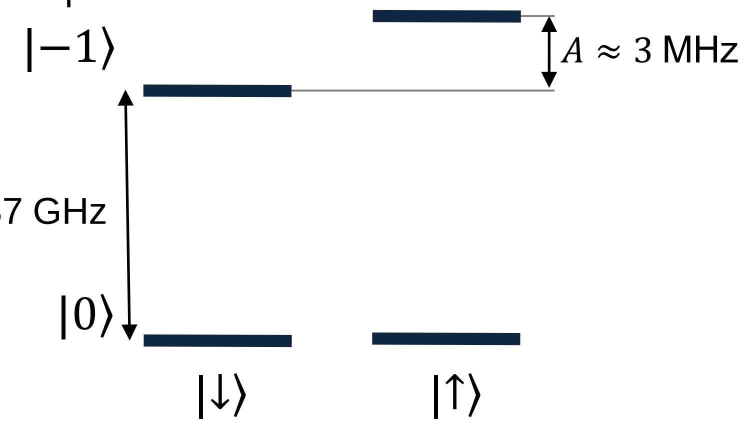

nuclear spin

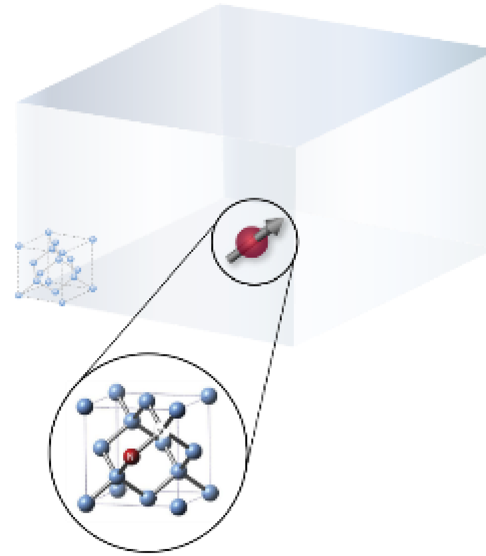

CNOT gate: flip electron spin conditional on nuclear spin state

⇩

SWAP electron spin state with nuclear spin state:

$$\alpha|0\rangle + \beta|-1\rangle \rightarrow \alpha|\downarrow\rangle + \beta|\uparrow\rangle$$

⇩

nuclear spin state is NOT destroyed by optical excitation ⇨ repetitive readout

D. Hume, et al.,
Phys. Rev. Lett. **99**, 120502 (2007)

Improving NV spin readout using quantum logic

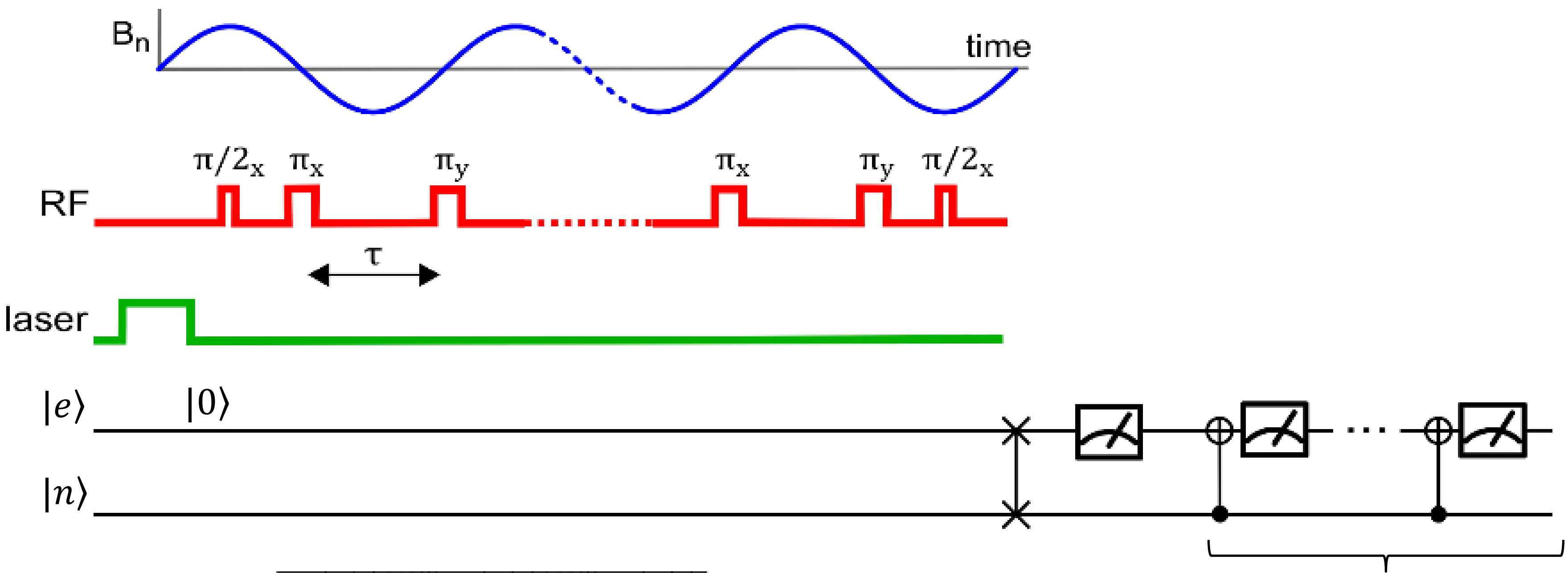

SWAP
$|e\rangle \leftrightarrow |n\rangle$

repetitive readout
of ^{15}N nuclear spin

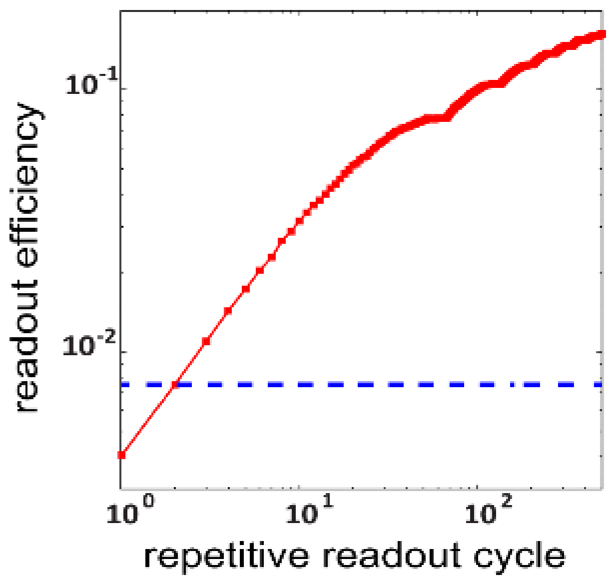

improved NV spin readout efficiency by ×30

Igor Lovchinsky, Alex Sushkov, Elana Urbach, Nathalie de Leon, et al.
manuscript in preparation

Single ubiquitin proteins

covalent attachment of ubiquitin protein to diamond surface:

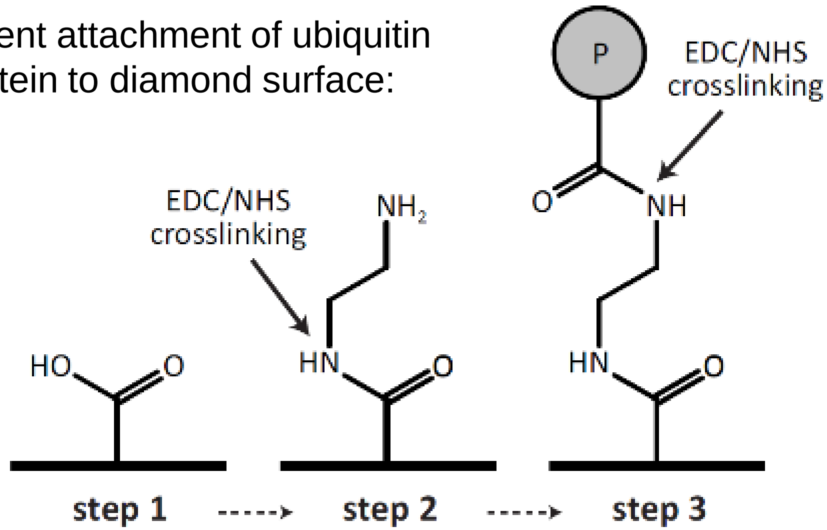

ubiquitin protein, enriched with ^{13}C $(I=1/2)$ and ^{2}H $(I=1)$

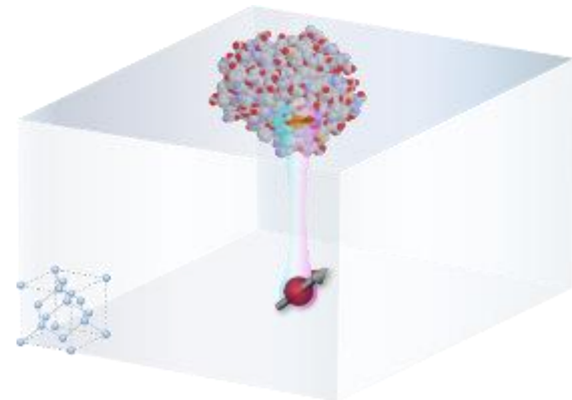

AFM of a clean diamond surface:

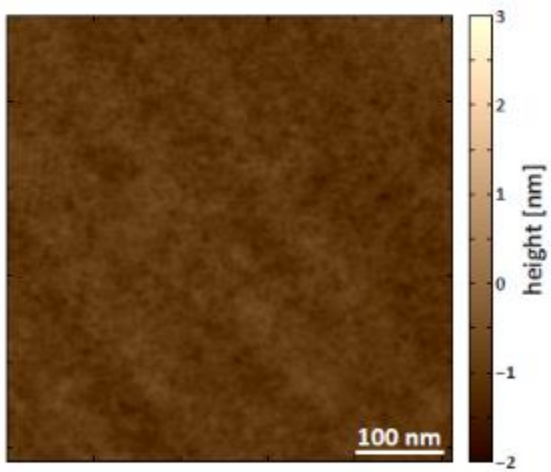

AFM of a diamond surface with attached proteins:

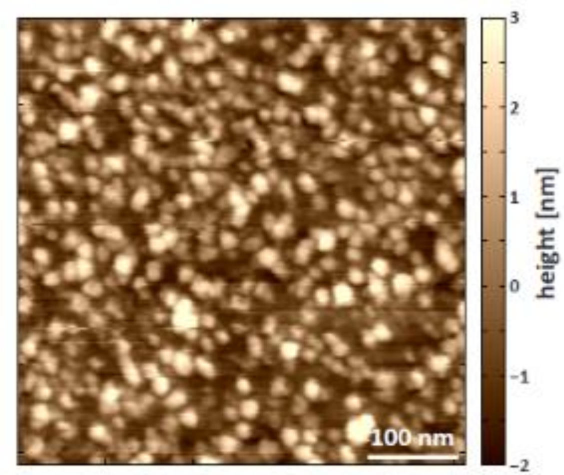

NMR spectroscopy on single ubiquitin proteins

use oxygen anneal diamond treatment and quantum logic-assisted NV spin repetitive readout

ubiquitin protein, enriched with ^{13}C (I=1/2) and ^{2}H (I=1)

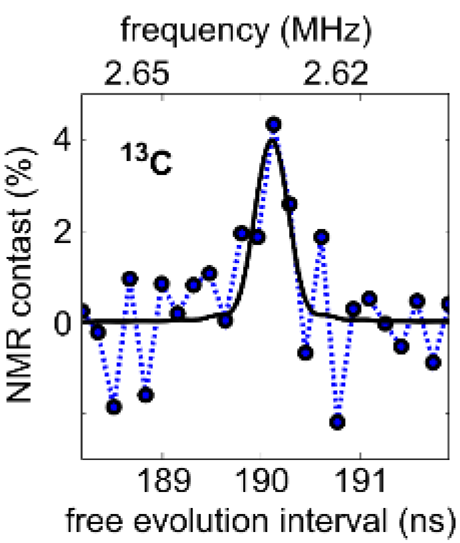

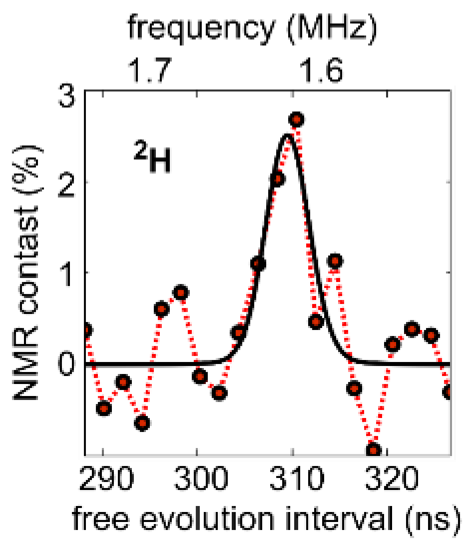

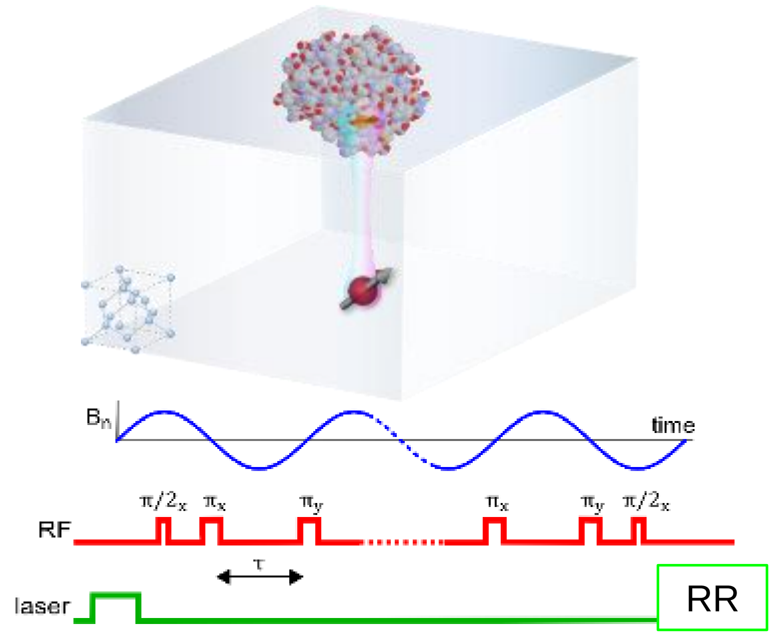

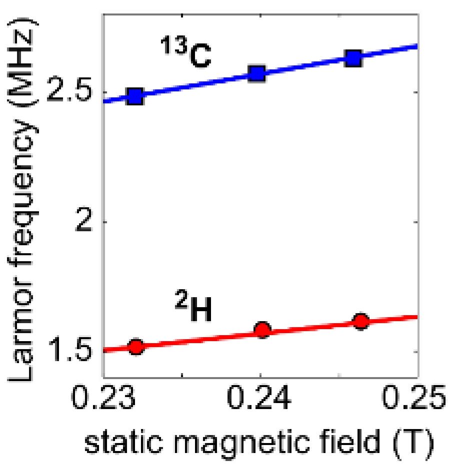

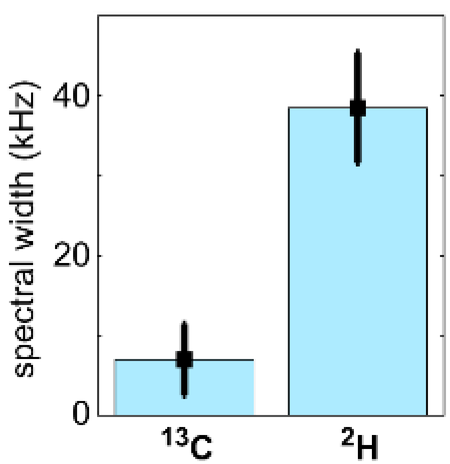

- ^{13}C linewidth consistent with dipolar broadening
- ^{2}H linewidth consistent with quadrupolar shifts → chemical environment

NMR with ≈ 400 nuclear spins in a single protein molecule

Igor Lovchinsky, A.S., Elana Urbach, Nathalie de Leon, et al.
manuscript in preparation

Outline

1. The NV color center in diamond: introduction and applications

2. Magnetic sensing with an NV center: the tools

3. NMR experiments with liquid hydrocarbons: detecting 10^4 nuclear spins

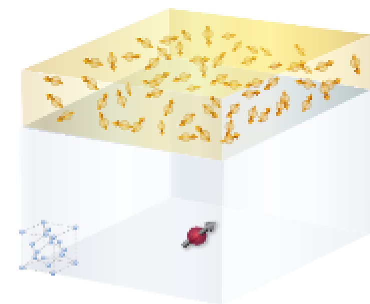

4. NMR spectroscopy of single protein molecules: detecting 400 nuclear spins

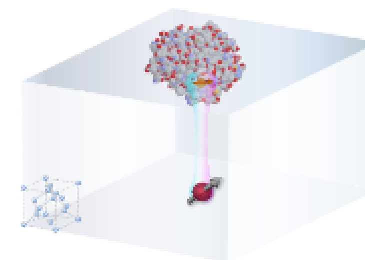

5. **NMR with single nuclear spin sensitivity**

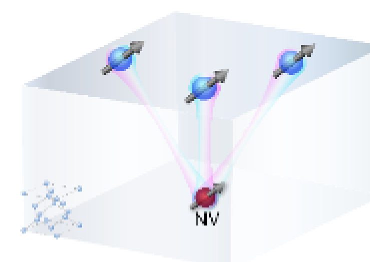

6. Outlook

Detecting single nuclear spins?

dipole field due to
single nuclear spin:

$$B_n \approx \frac{\mu_n}{r^3}$$

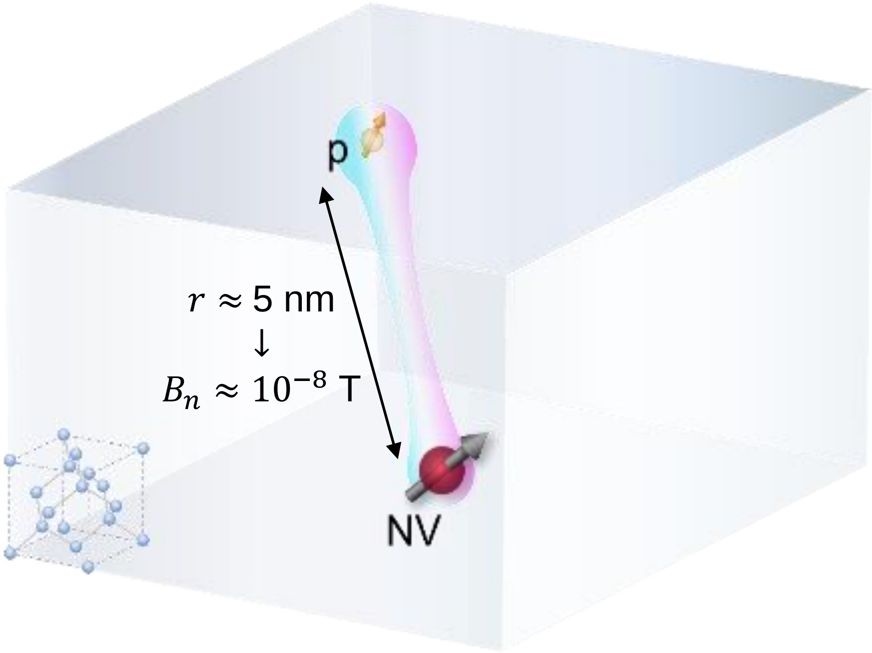

surface nuclear spin → NV center → optical readout

Diamond surface electron spins

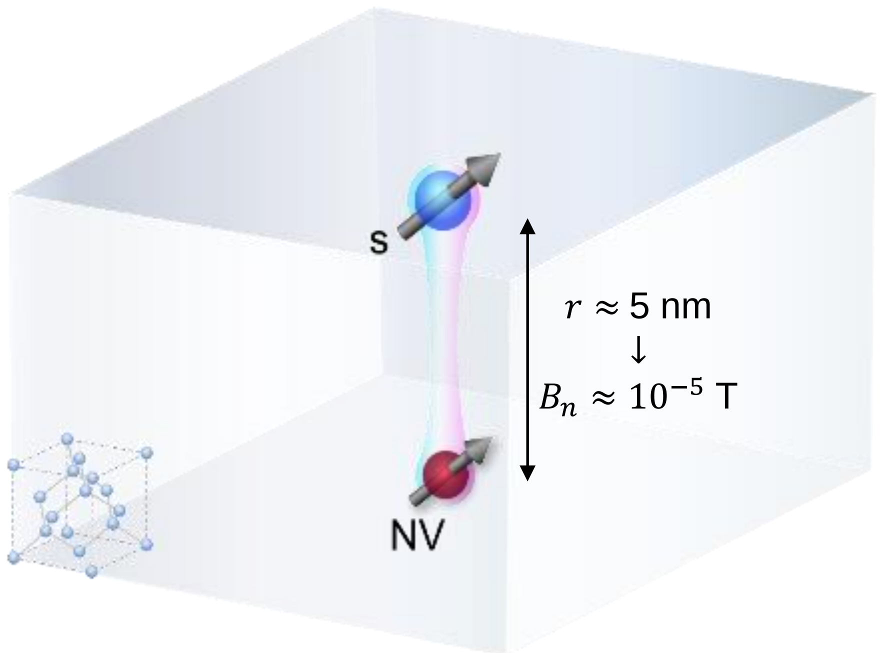

dipole field due to single electron spin:

$$B_e \approx \frac{\mu_e}{r^3}$$

surface electron spin → NV center → optical readout

M. Schaffry et al., *Phys. Rev. Lett*. **111**, 207210 (2011)

Idea: reporter-assisted nuclear spin sensing

dipole field due to single nuclear spin:

$$B_n \approx \frac{\mu_n}{r^3}$$

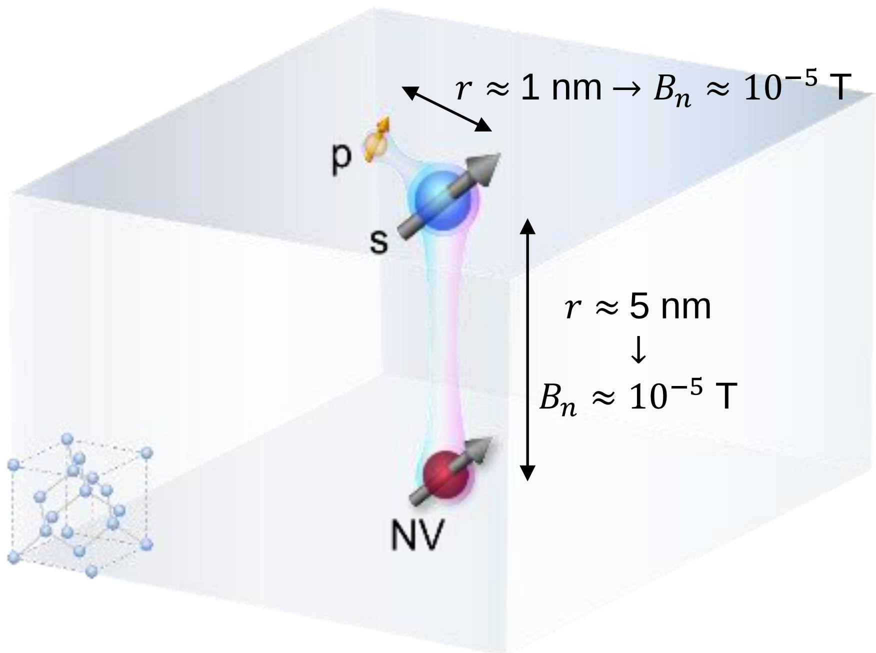

dipole field due to single electron spin:

$$B_e \approx \frac{\mu_e}{r^3}$$

surface nuclear spin → reporter electron spin → NV center → optical readout

<u>idea</u>: surface electron spins →
magnetic “reporters” directly on the surface

Detection of diamond surface electron spins

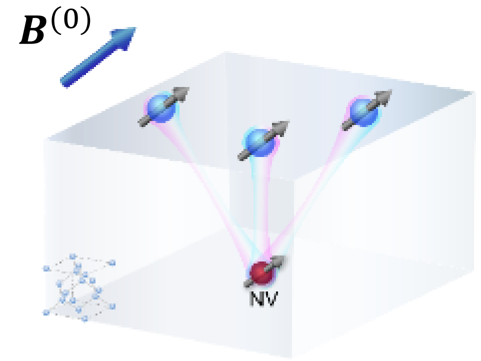

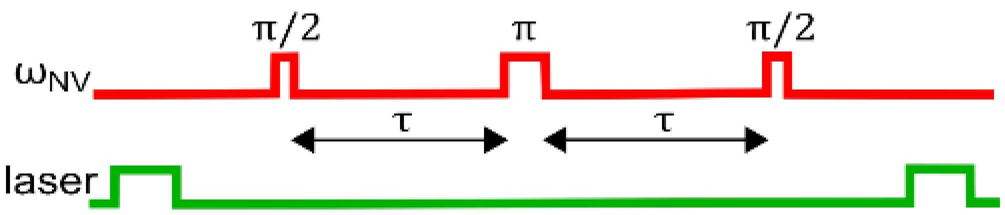

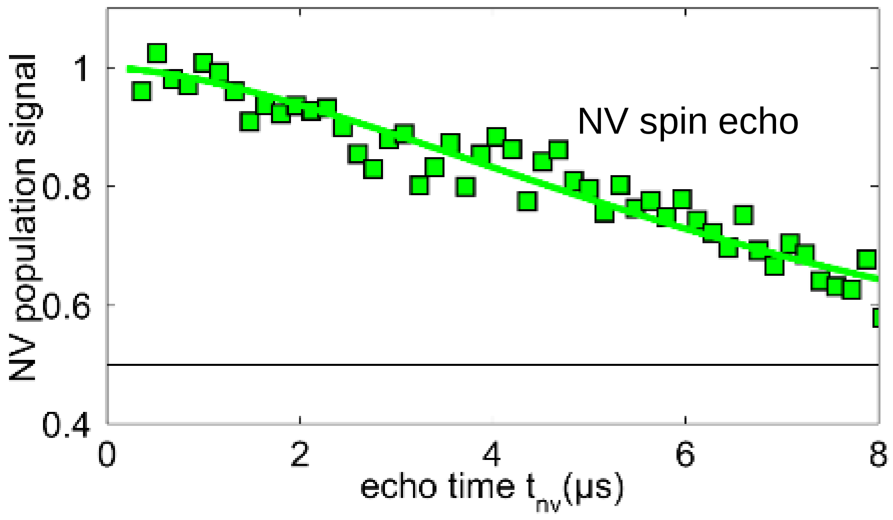

Detection of diamond surface electron spins

DEER: Double Electron-Electron Resonance

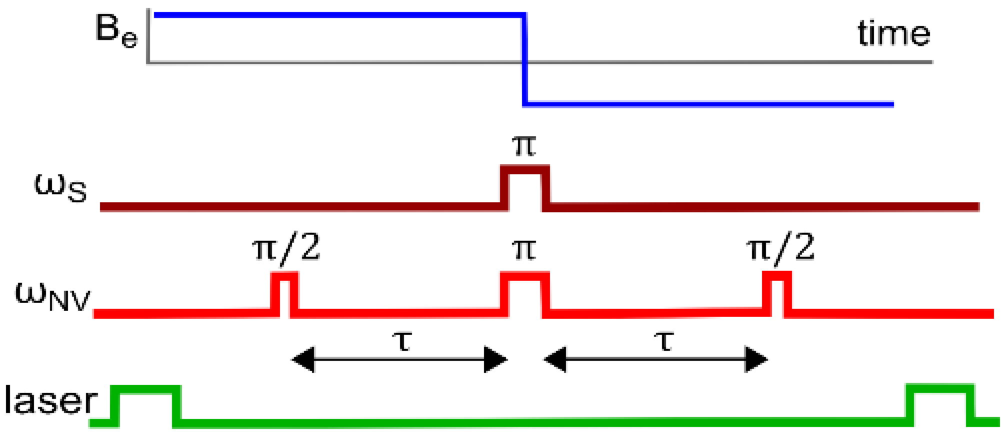

$\varphi_1 + \varphi_2 \propto 2B_e\tau$

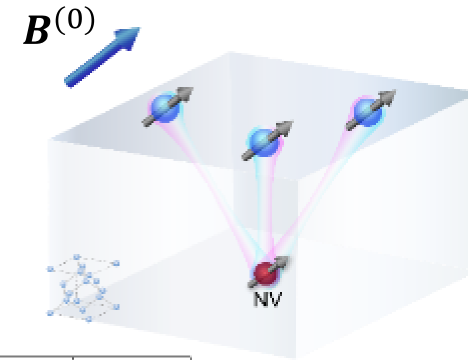

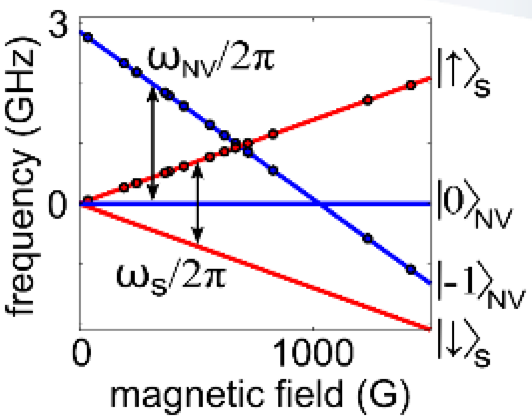

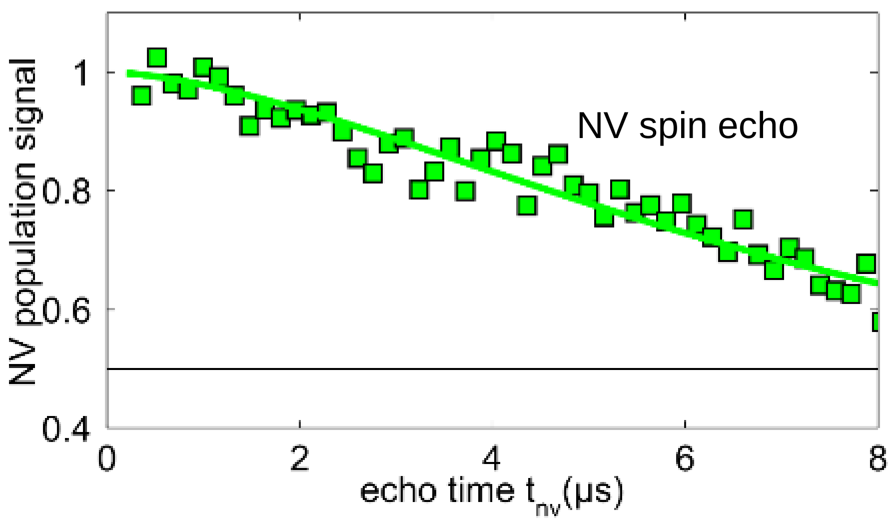

M. Grinolds et al.,
Nature Nano. **9**, 279(2014)

Detection of diamond surface electron spins

DEER: Double Electron-Electron Resonance

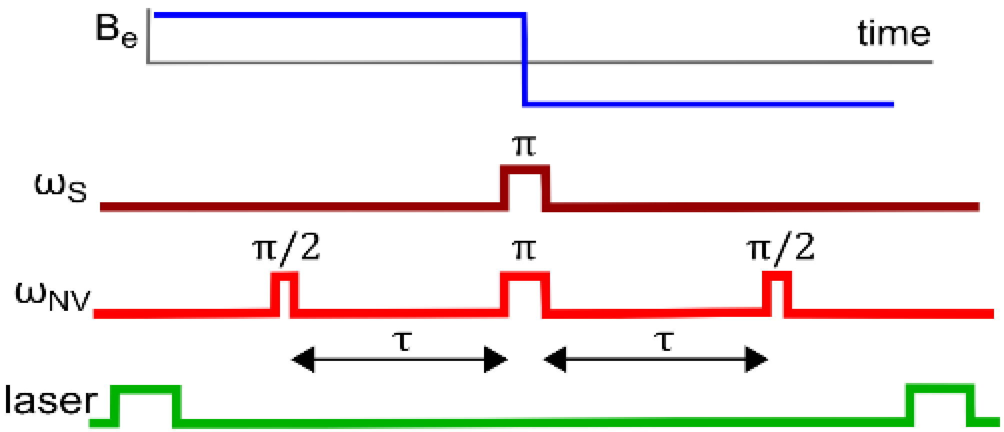

$$\varphi_1 + \varphi_2 \propto 2B_e\tau$$

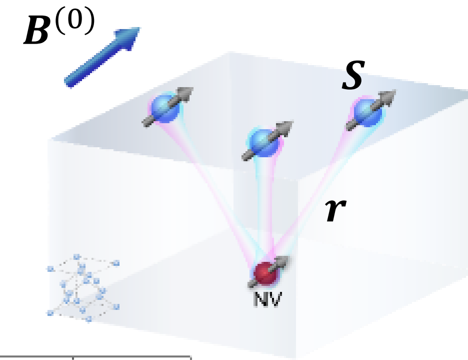

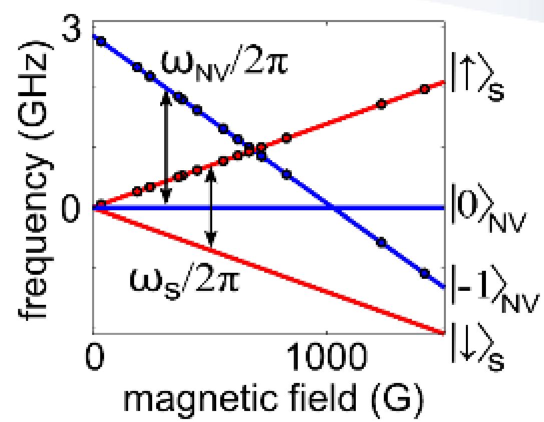

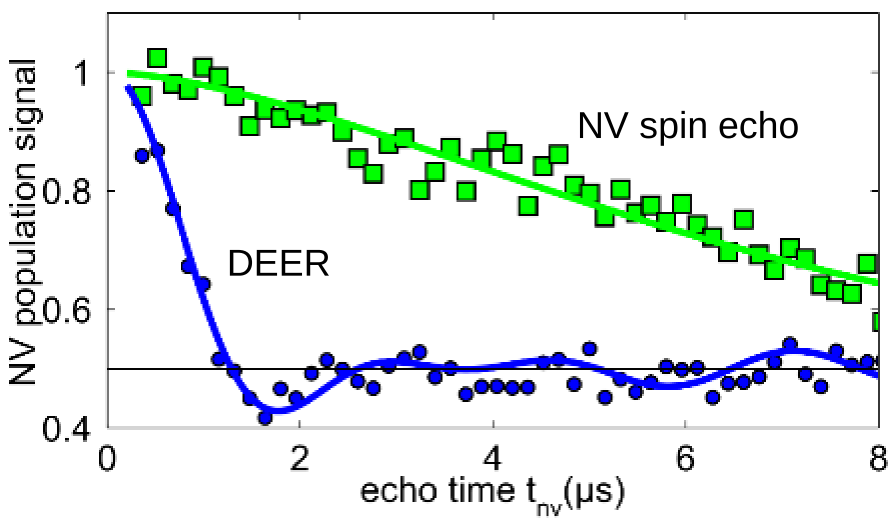

magnetic field created at NV location by electron spin $\boldsymbol{S}$:

$$B_e = \frac{g\mu_B}{r^3}\left[\boldsymbol{S} - 3\frac{(\boldsymbol{S}\cdot\boldsymbol{r})\boldsymbol{r}}{r^2}\right]$$

B_e → DEER decay

M. Grinolds et al., *Nature Nano*. **9**, 279(2014)

Imaging of diamond surface electron spins

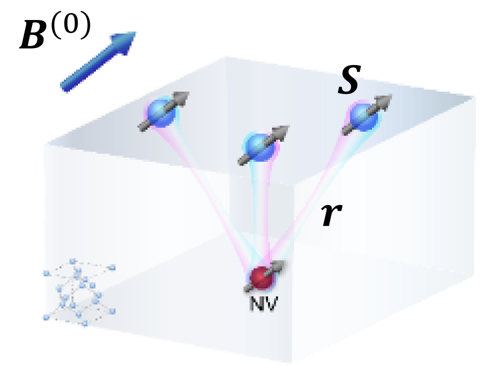

idea:

$$B_e = \frac{g\mu_B}{r^3}\left[\boldsymbol{S} - 3\frac{(\boldsymbol{S}\cdot\boldsymbol{r})\boldsymbol{r}}{r^2}\right]$$

depends on angle between static magnetic field and $\boldsymbol{r}$

DEER measurements at several different directions of static magnetic field ⇒

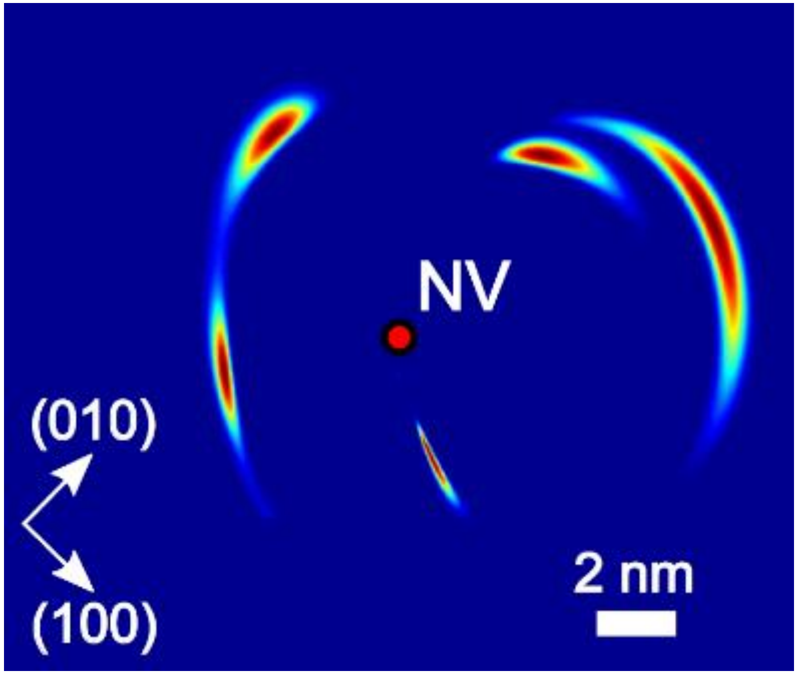

determine locations of surface electron spins with nanometer uncertainty

Alex Sushkov, Igor Lovchinsky, et al., *Phys. Rev. Lett*. **113**, 197601 (2014)

Manipulation of diamond surface electron spins

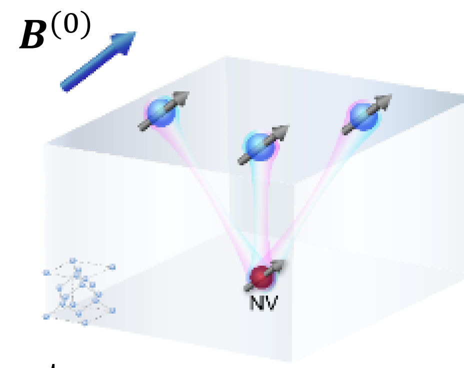

idea: "reporter" pulse sequence →
measures change in surface electron spin state

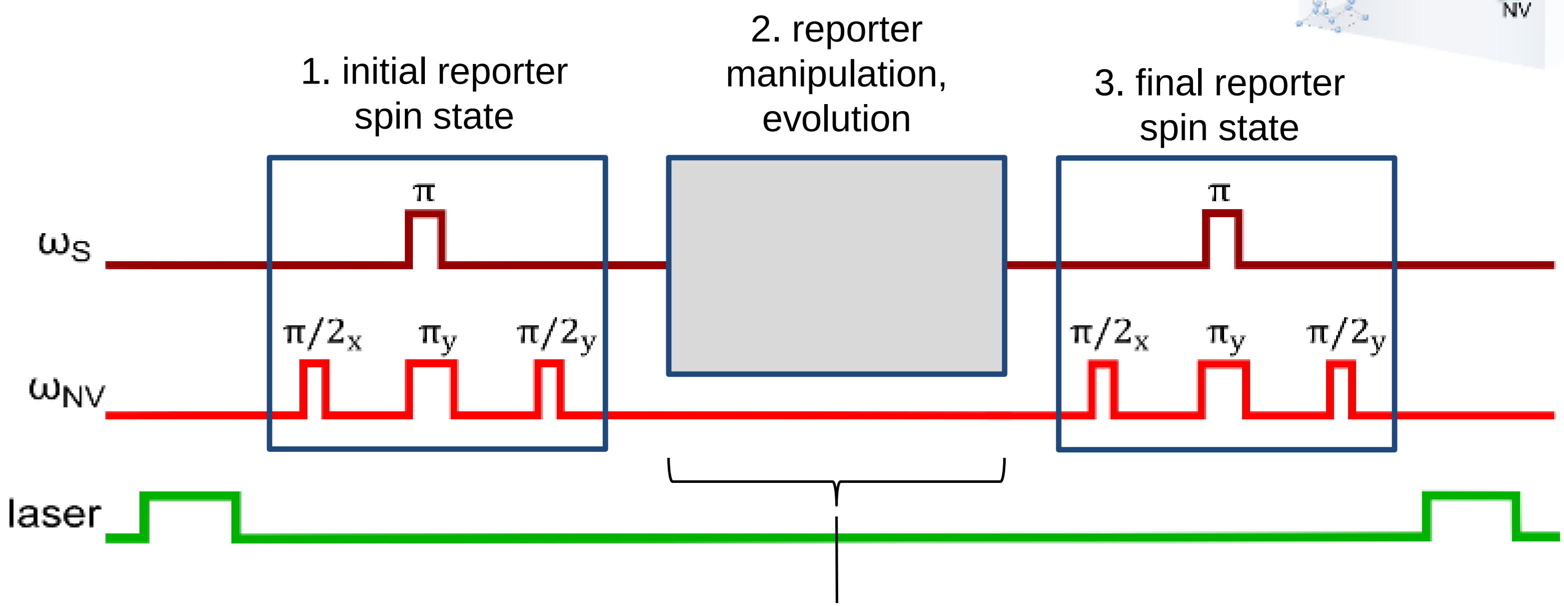

information is stored
in NV spin population

⇩

not affected by NV spin decoherence

A. Laraoui et al.,
Nature Comm. **4**, 1651 (2013)

Coherent control of diamond surface electron spins

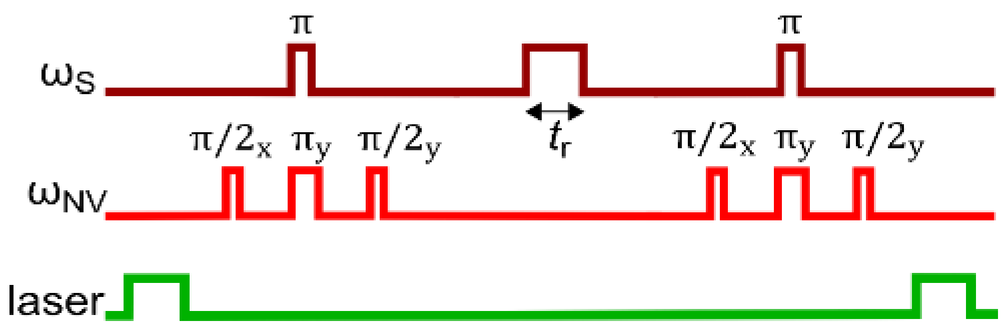

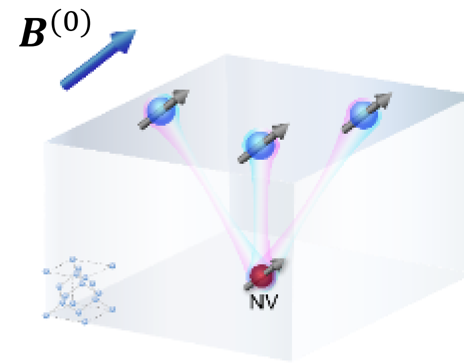

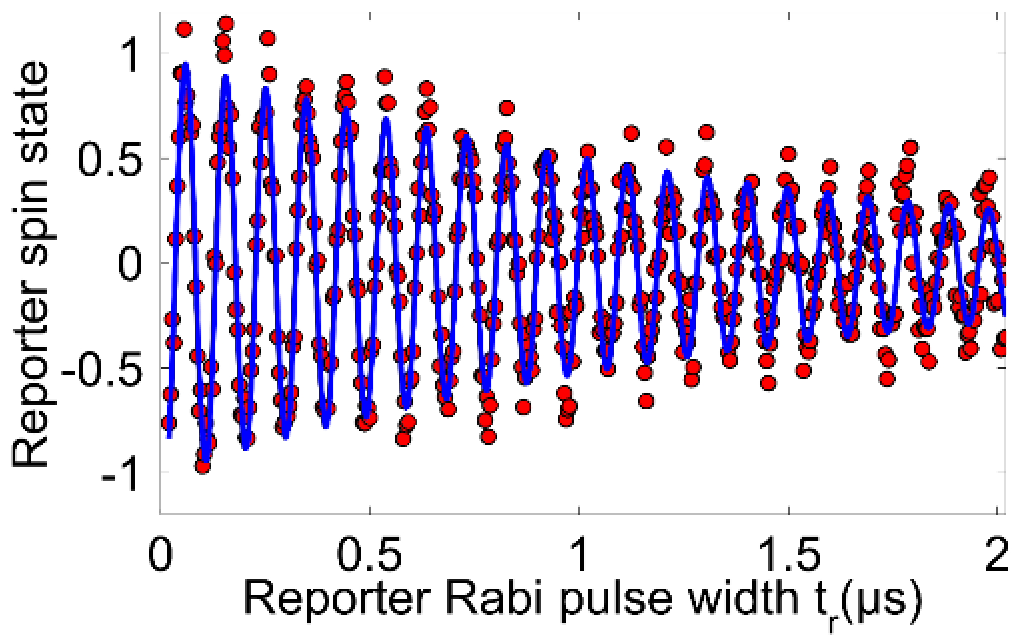

Rabi oscillations

coherent control of surface electron spin state

Using surface electron spins as magnetic reporters to detect proton spins

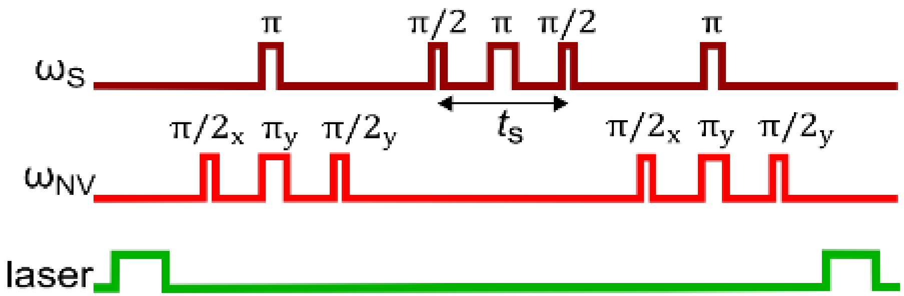

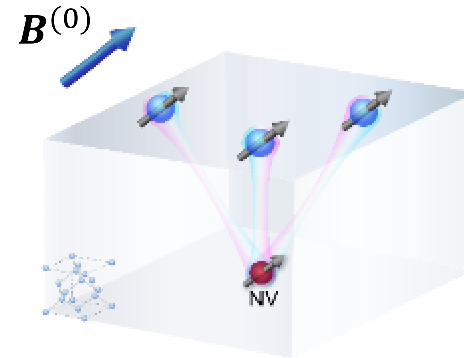

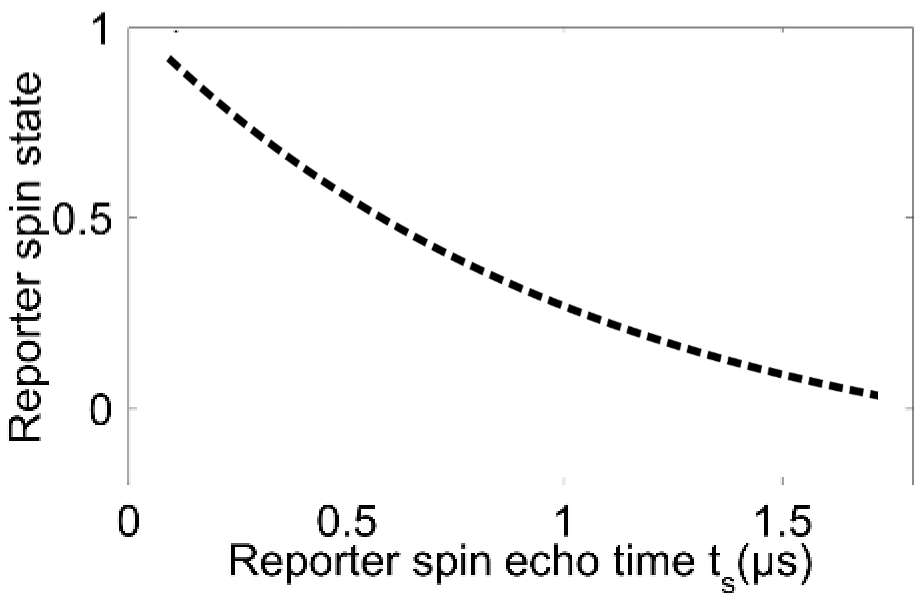

Larmor

$$H_n = g_n \mu_n I_z B_z^{(0)}$$

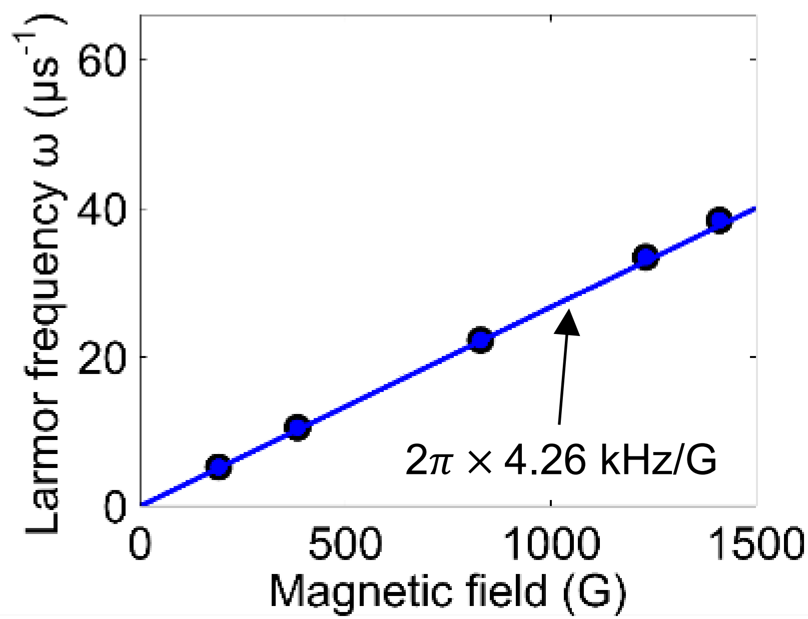

detecting surface proton spins using electron-spin reporters

Coherent coupling between surface electron spins and proton spins

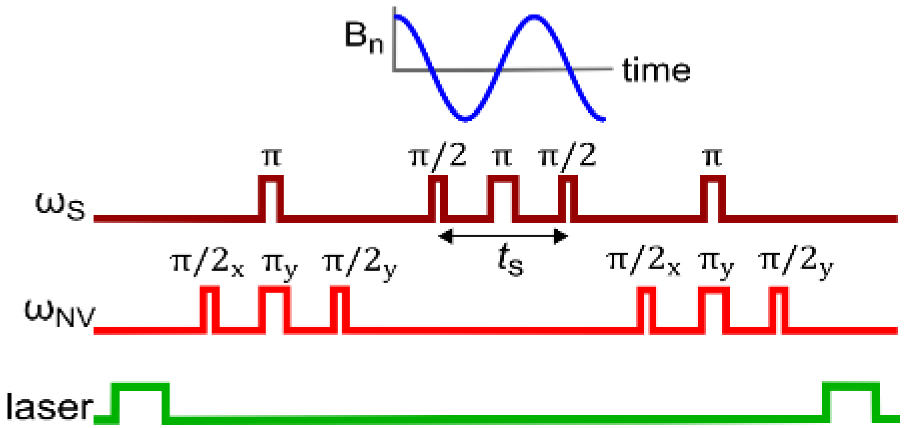

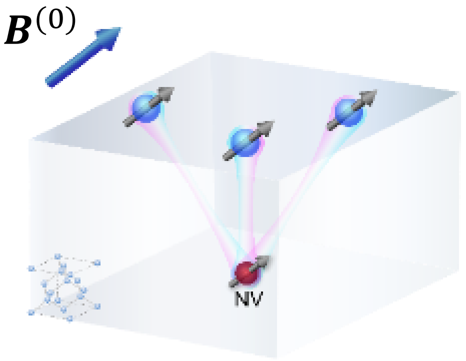

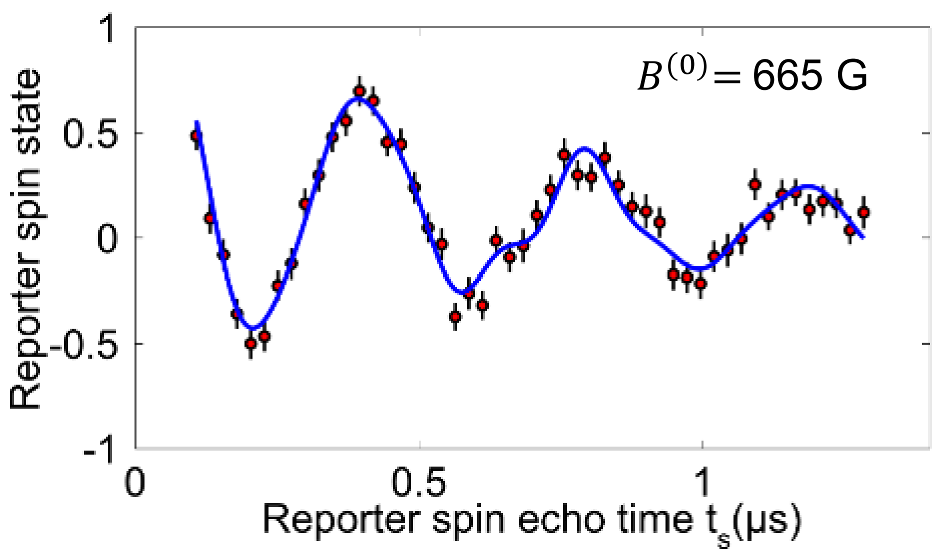

Larmor + hyperfine

$$H_n = g_n \mu_n I_z B_z^{(0)} + a I_z S_z + b I_x S_z$$

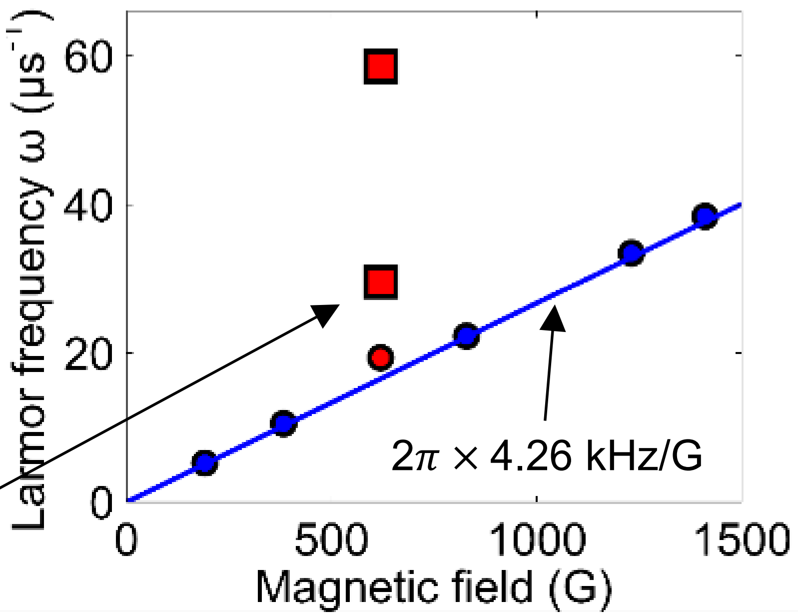

coherent hyperfine coupling between protons and reporters

Coherent coupling between surface electron spins and proton spins

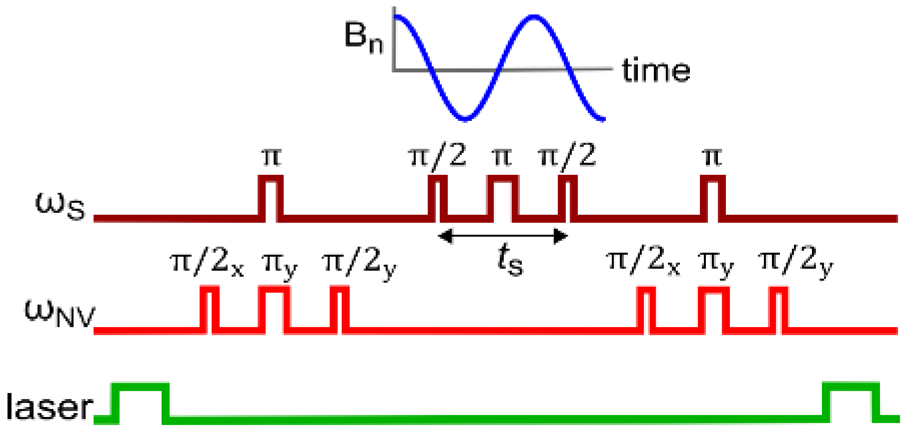

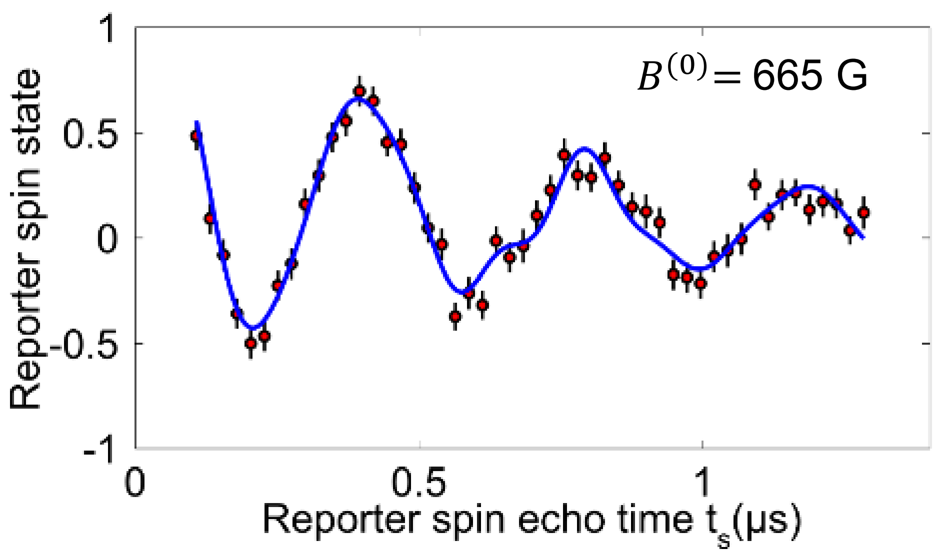

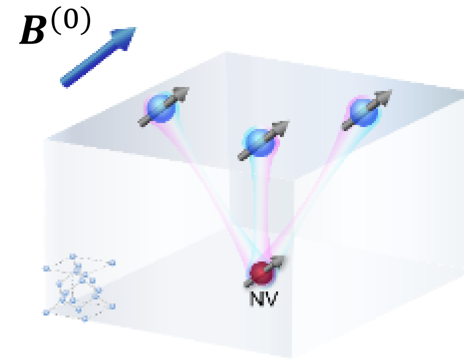

Larmor + hyperfine

$$H_n = g_n \mu_n I_z B_z^{(0)} + a I_z S_z + b I_x S_z$$

extract hyperfine parameters a, b

hyperfine interaction: dipole-dipole + contact

extract proton position relative to surface electron spin

Localization of individual coherently-coupled protons

polar plot, no azimuthal angle information

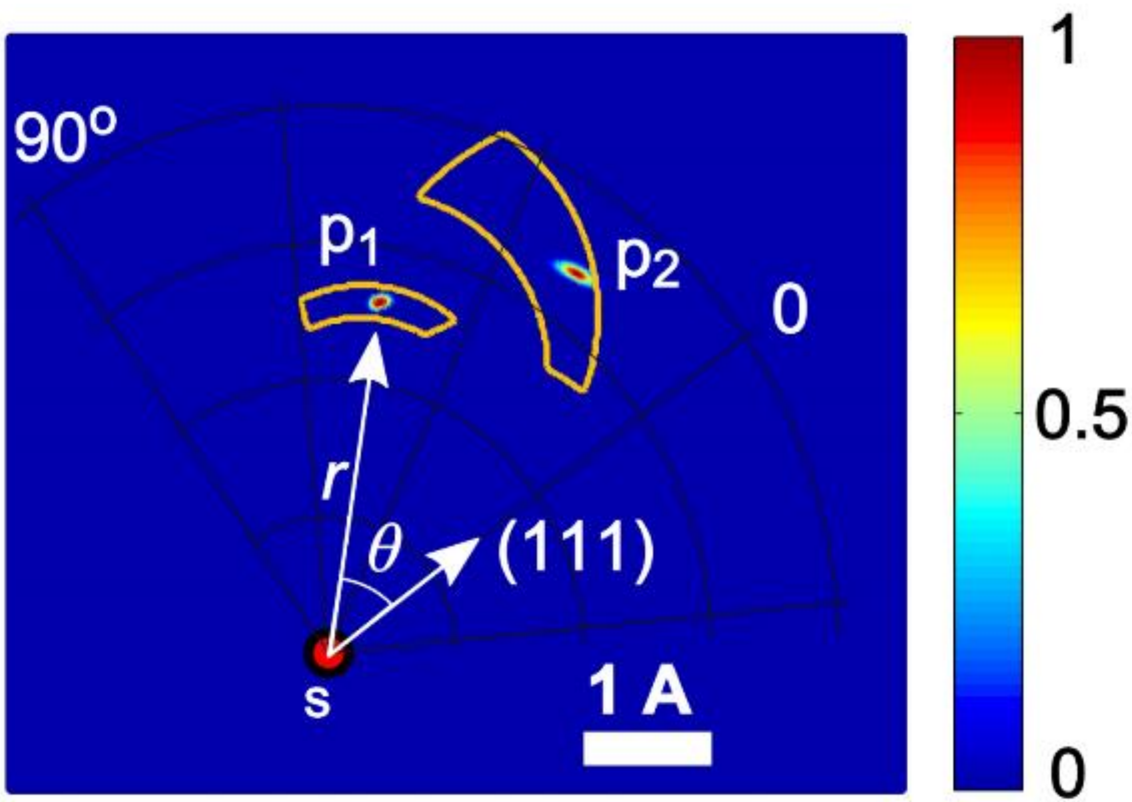

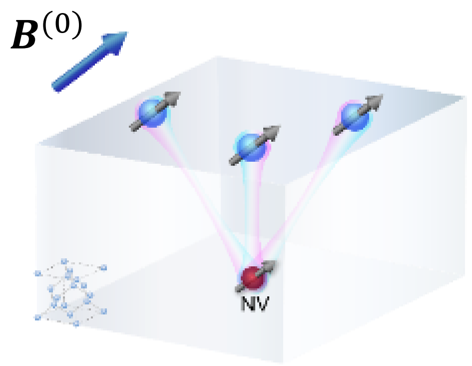

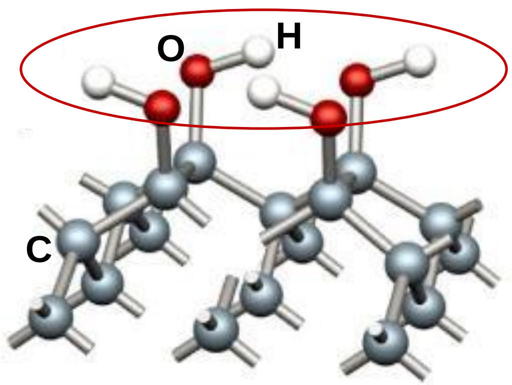

detection and localization of the surface proton spins relative to the reporter spin

Alex Sushkov, Igor Lovchinsky, et al., *Phys. Rev. Lett.* **113**, 197601 (2014)

Taking magnetic sensing to the nanoscale

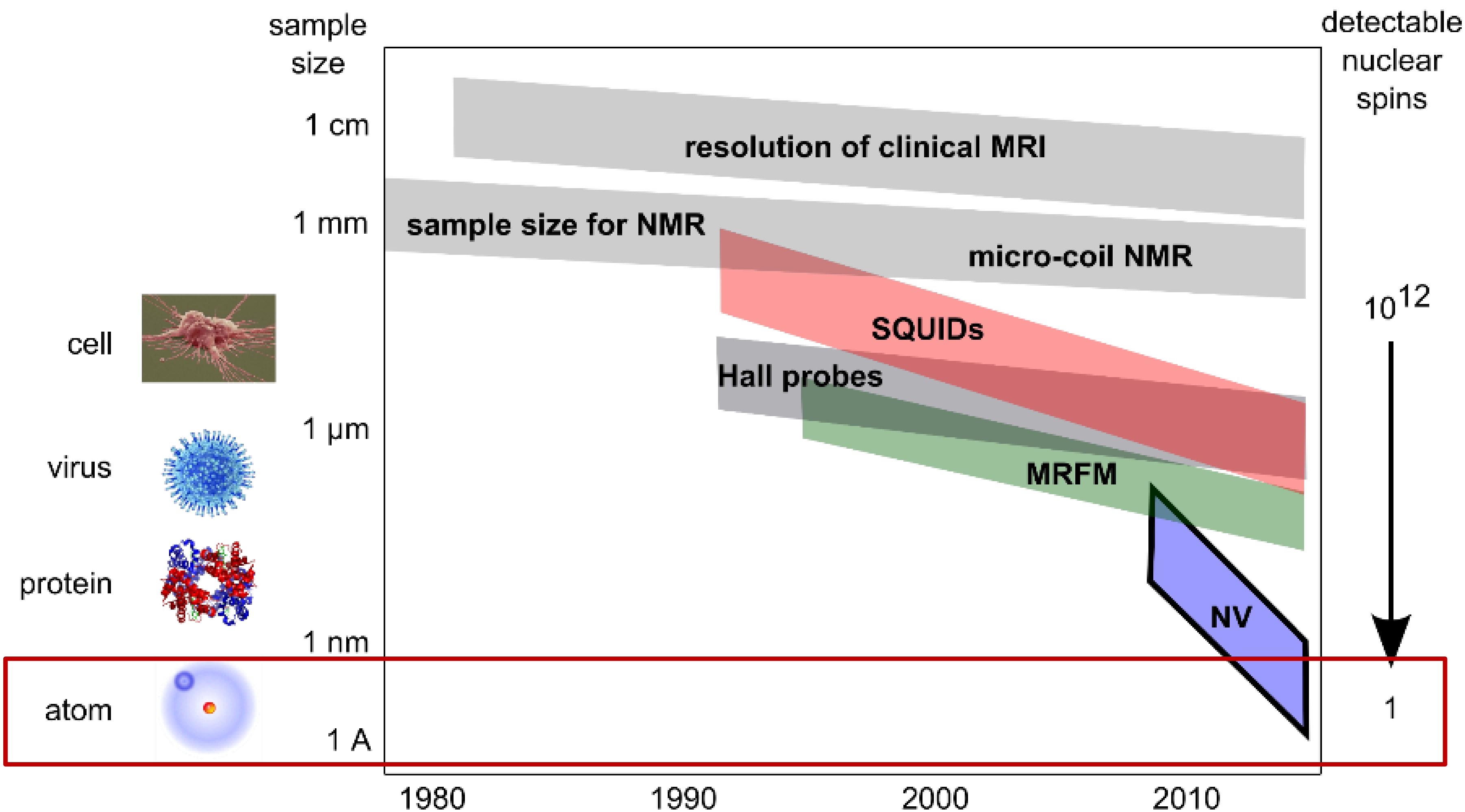

Outlook

single-molecule magnetic tomography
(coherent quantum dynamics between nuclear spins in the molecule)

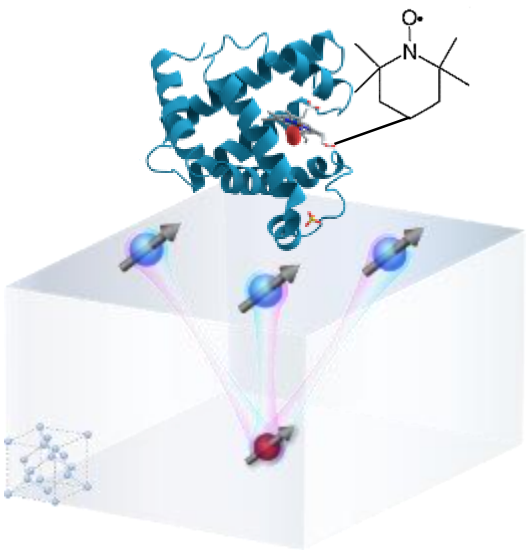

[*Phys. Rev. X* 5, 011001 (2015)]

nanoscale magnetic fields near surfaces

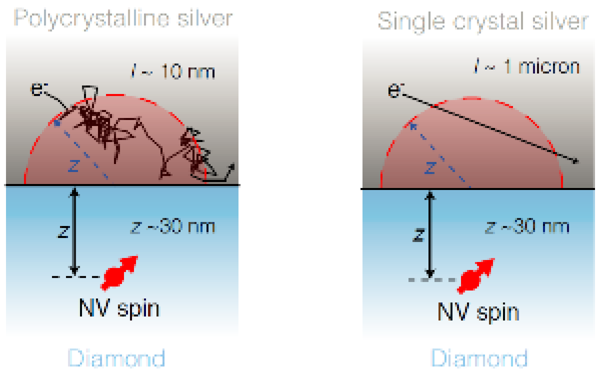

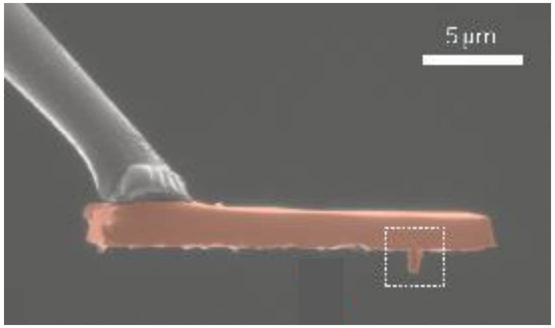

[*Nature Nano.* 9, 279 (2014)]
[*Nature Phys.* 9, 215 (2013)]
[*Nature Nano.* 7, 320 (2012)]
[Phys. Rev. Appl. 2, 054014 (2014)]

Outlook: addressable interacting spin systems

interplay between dynamics, interactions,
and disorder in dipolar spin systems
(many-body localization?)

quantum simulation?

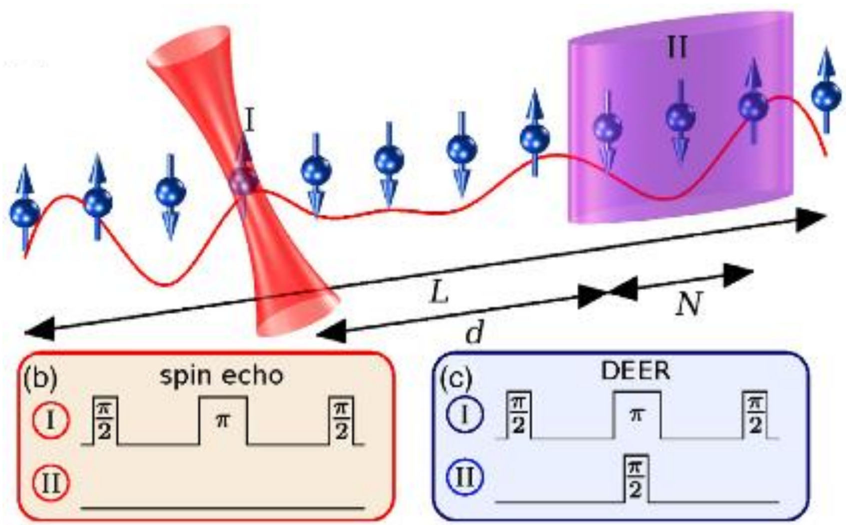

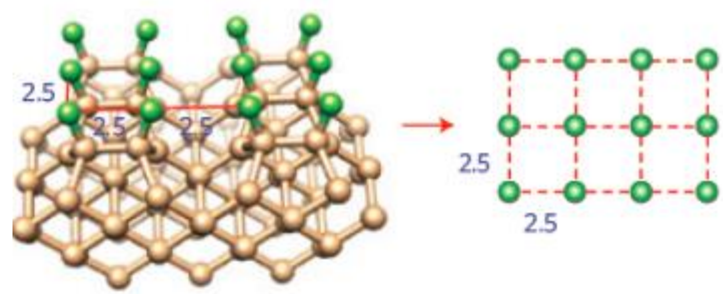

[Nature Phys 9, 168 (2013)]

[*Phys. Rev. Lett*. **113**, 147204 (2014)]
[*Phys. Rev. Lett.* **113**, 243002 (2014)]

Outlook: the nature of dark matter?

<u>idea</u>: solid-state spin qubits for an axion dark matter search

axion dark matter induces oscillating energy shifts for nuclear spins inside a solid sample (oscillation frequency = axion mass)

search for signature of such shifts in a magnetic resonance experiment, by tuning the external magnetic field

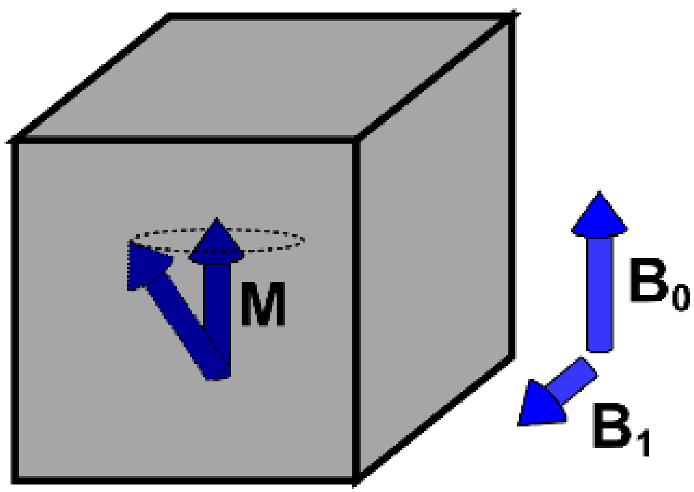

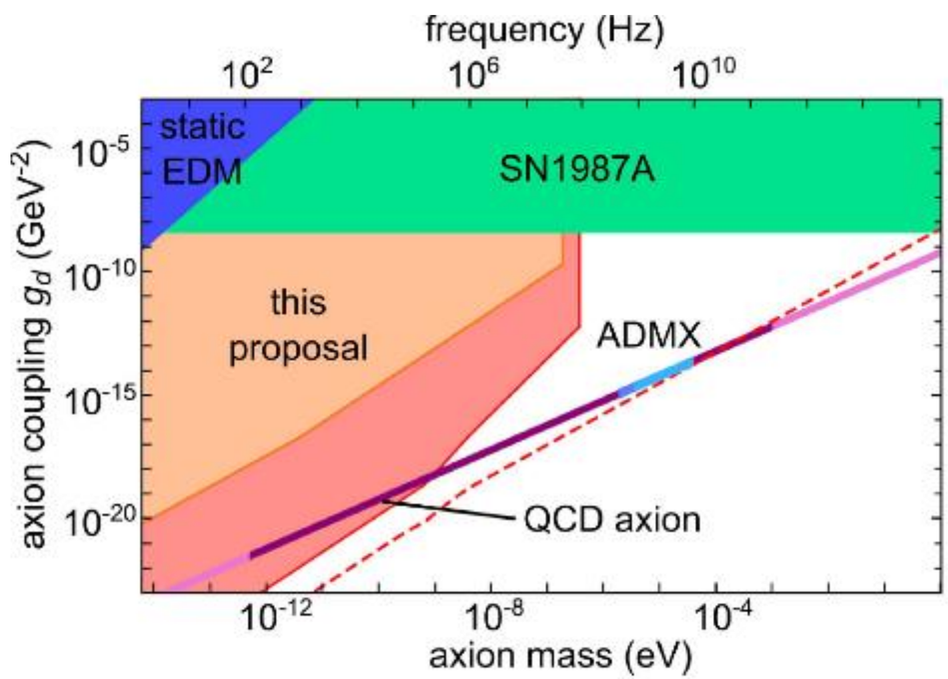

[D. Budker, P.Graham, et al., *Phys. Rev. X* **4**, 021030 (2014)]

Summary

NMR experiments with liquid hydrocarbons: detecting 10^4 nuclear spins → 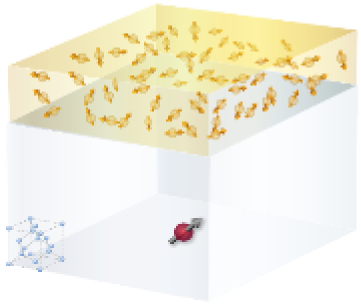

NMR spectroscopy of single protein molecules: detecting 400 nuclear spins → 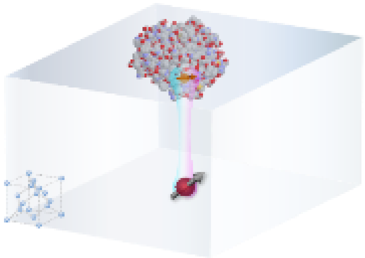

NMR with single nuclear spin sensitivity → 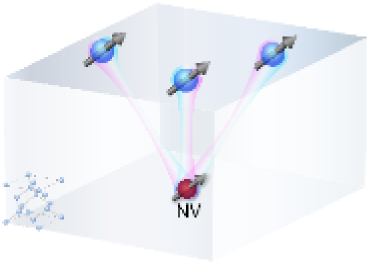

Thanks !

Nathalie de Leon
Ruffin Evans
Kristiaan de Greve
Shimon Kolkowitz
Arthur Safira
Quirin Unterreithmeier
Georg Kucsko
Peter Maurer
Alp Sipahigil
Sasha Zibrov
Jeff Thompson
Thibault Peyronel
Crystal Senko
Mike Goldman

Igor Lovchinsky
Elana Urbach
Nick Chisholm
My Linh Pham
Stephen DeVience
Chinmay Belthangady
Emma Rosenfeld
Sonwoon Choi
Eric Kessler
Peter Komar
Norman Yao
Steve Bennett
Brendan Shields
Yiwen Chu

Marsela Jorgolli
Peggy Lo
Minako Kubo
Alex High
Rob Devlin
Alan Dibos
Tianyang Ye
Mark Polking
Alex Shalek
Ashok Ajoy
Luca Marseglia
Saha Kasturi
David Hunger
Alexei Akimov

Misha Lukin

Hongkun Park

Ron Walsworth

Paola Cappellaro

Amir Yacoby